HYGROSCOPIC EFFECTS ON PAPERBOARD CORES AND WOUND ROLLS

By

HUNG VU NGUYEN

Bachelor of Science
Oklahoma State University
Stillwater, Oklahoma

1995

Submitted to the Faculty of the
Graduate School of the
Oklahoma State University
in partial fulfillment
of the requirements for
the Degree of
MASTER OF SCIENCE
December, 1997

HYGROSCOPIC EFFECTS ON

PAPERBOARD CORES AND

WOUND ROLLS

Thesis Approved

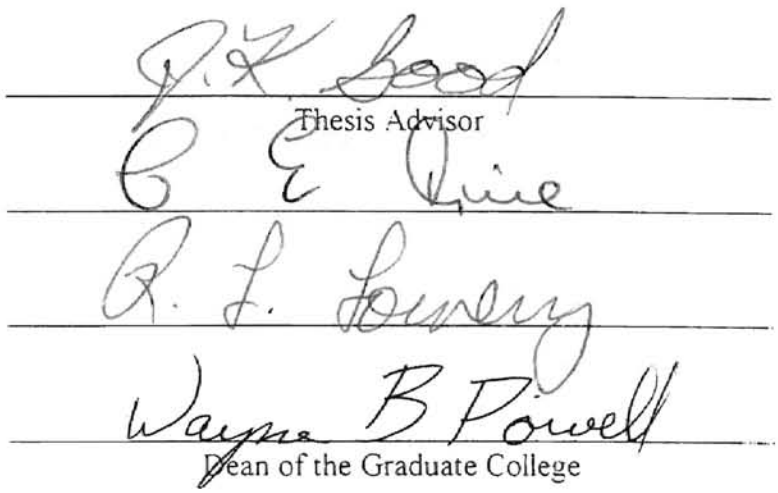

Thesis Advisor

Dean of the Graduate College

ACKNOWLEDGMENTS

I would like to thank Dr. Good for his help and encouragement throughout the development of this topic. There were times when I thought this paper would never get finished. Thank you Dr. Good for all your patience. I will never forget your help and encouragement.

Additionally, I would like to thank Robert Steves, Noman Ahmad, Russell Cullens, Trang Nguyen, and Kevin Wehba for being there when I needed help whether there for technical help or just keeping my mind on my work. Their company was highly appreciated. I like to thank Ron Markum and Robert Taylor for their knowledge and technical support. Their help and ideas were invaluable. I would like to give special thanks to Jeff Henning for helping me with the viscoelasticity portion of this research.

Finally, I would like to thank my parents, Son & Que Nguyen, whose love made this possible.

TABLE OF CONTENTS

LIST OF TABLES

LIST OF FIGURES

NOMENCLATURE

A_1, A_2, A_3, A_4	humidity compliance coefficients
c	thickness of cantilever beam
c_{brass}	thickness of brass shim
D_i	radial deformation inward
ΔD	change in core diameter
Δ(DCDT)	displacement reading of DCDT
E	elastic modulus
E_r	radial modulus
E_t	tangential modulus
E_{brass}	brass elastic modulus
E_{cm}	modulus of core material
E_c	core stiffness
F	punch force
g^2	E_t/E_r
h(t)	Heaviside step function
H(t)	humidity compliance function
J(t)	creep compliance function
J_0, J_1, J_2	creep compliance coefficient
L	length of cantilever beam

P	pressure
δP	incremental pressure
δP_i	incremental pressure at lap i
R	linear spring constant
r	roll radius
r_i	radius at lap i
r_{last}	radius of wound roll
r_{out}	outer radius of core
r_{in}	inner radius of core
r_{slip}	radius punch force was applied
s	Laplace transform operator
ΔT	temperature change
t	time
W	width of cantilever beam
w	width of web
Wt	core weight
α_c	core coefficient of thermal expansion
α_t	radial coefficient of thermal expansion
α_r	tangential coefficient of thermal expansion
ε	strain
ε_{brass}	strain of brass strip
ε_{DCDTu}	strain of core due to humidity change

ε_{DCDTr}	strain of core under brass shim
ε_1	strain of spring element
ε_2	strain due to viscosity
ε_0	initial strain on viscoelastic material
ε_t	tangential strain
ε_r	radial strain
σ	stress
σ_o	initial stress on viscoelastic material
σ_r	radial stress
σ_t	tangential stress
τ_1, τ_2	relaxation time
υ	Poisson's ratio
υ_c	Poisson's ratio of core
μ_s	coefficient of friction
χ	change in percent moisture content

CHAPTER 1

Introduction

A web is a thin continuous material with little or no bending stiffness. Web materials include plastic film, paper, fabric, and thin metals. The method of processing and transporting this material is called web handling. A web is usually transported along rolls. The rolls can be free spinning or driven. The final rolls in the process usually include cores, on which the web is wound. The cores, hollow cylinders easily mounted on expanding mandrels on a winder or an unwinding module, are made of many different materials: paper, plastic, steel, or aluminum. A large percentage of cores are composed of paper fibers, resins and adhesives. These cores are considered to be disposable. Manufacturers of base web materials often ship their paper or film webs in wound roll format to web converters who process the web into the final product. Manufacturers will ship their web on the cheapest core available that will withstand the pressures due to winding. The web converter will dispose of the cores after an unwinding roll of the web has been expended. Plastic or metal cores are used but only in high value products, such as data cartridges or in-plant operations, where the cores are recovered.

Web handling strives to maintain a high quality of a wound roll. In order to do this, stresses within the wound roll must be known. Knowing the stress leads to effective packaging of the web. It helps prevent high stress, which could damage the web, or low

stress, which could cause problems in unwinding. For these reasons, it is important to establish a good model of the stresses that can develop within the roll.

For the economic reasons mentioned, most wound rolls are shipped and stored on paperboard cores. One problem with using paperboard is that it will take on, and give up, moisture until it reaches equilibrium with the environment. This moisture change also causes changes in the dimensions of paperboard. This dimension change of the core will cause changes in the stress of the wound roll. Therefore, the objective of this research is to develop a model for a wound roll that incorporates the effect of moisture on the paper core. The model will predict how stresses in the wound roll change through time due to changes in humidity.

CHAPTER 2

Literature Survey

Rule of Thumb

A survey of the literature was done to see if there was any previous study pertaining to moisture effects on paperboard cores. The research did find one article that pertains to this problem. The article was published by Composite Can and Tube Institute (CCTI) [2]. The article delineates a "rule of thumb" guideline for estimating dimension changes due to moisture. The article states that for each percentage unit change in tube moisture content, the tube would change its dimension by the following amount:

Length	.12%
Outside Diameter	.09%
Wall thickness	.6%
Inside Diameter	.03%

Table 2.1: "Rule of Thumb" for estimating dimensional changes of paperboard core

Increases in moisture content causes increased dimensions; decreases in moisture content results in decreased dimensions. For example, a three-inch outside diameter core that experiences a 10% change in its moisture content will grow to approximately 3.027 inches: $(3\times.0009\times10)+3.=3.027.$

Moisture Content

Paperboard is made of cellulose, which is hydrophilic and will easily give up and take on moisture from the environment. It will do this until it reaches equilibrium, a point where it is neither gaining or losing moisture to the air. The moisture content of cellulose materials usually ranges from 3% to 18%. The moisture content is controlled by the surrounding air relative humidity (RH), rather than the water content of the air (absolute humidity). The table below shows the moisture content of paperboard due to different RH according to CCTI [2].

Relative Humidity	Percent Moisture
10%	2.8%
20%	4.0%
30%	5.2%
40%	6.0%
50%	7.5%
60%	9.0%
70%	10.5%
80%	13.0%
90%	16.0%

Table 2.2: Relative humidity vs. Percent Moisture (Paperboard)

The values listed above can vary depending on material, product density, and on whether the paperboard is taking on or giving off moisture as it attains equilibrium. Paperboard will reach a different equilibrium depending on whether it is drying or wetting. The differences can range from 1 to 2 percent.

Humidity

Environmental moisture is the most important condition affecting paperboard dimension. Environmental moisture is usually measured by either absolute humidity or relative humidity. The preferred way to measure it, in relation to how air takes on and gives up moisture and how paperboard takes on and gives up water, is relative humidity. Air can hold only a certain amount of moisture depending on the temperature. Relative humidity is the ratio of the moisture in the air to the maximum amount of moisture the air can hold at any given temperature. Relative humidity is affected by temperature. Small changes in temperature can have significant changes in the amount of water that air can hold. For example, at 70°F one kilogram of air can hold 15.6 grams of water vapor. When the temperature rises to 80°F, one kilogram of air can hold 27.9 grams of water. Therefore, 100 percent relative humidity (RH) air at 70°F drops to 68% RH when the temperature rises to 80°F, if no additional moisture is available. It is conceivable, then, that a paperboard core could encounter a wide ranging RH, due to transportation and seasonal changes. This is especially true during winter when there is a large difference between inside and outside temperatures. Table 2.3 shows the indoor RH when the outside air is 75% RH at different temperatures for indoor temperature of 70°F, 75°F, and 80°F.

Outdoor Temperature (°F)	Indoor Temperature 70°F	75°F	80°F
-20	1.5% RH	1.3% RH	1.1% RH
-10	2.5	2.5	1.9
0	4.4	3.8	3.2
10	7.2	6.2	4.3
20	11.6	9.9	8.4
30	18.1	15.5	13.2
40	26.8	22.7	19.5
50	38.3	32.6	27.9
60	54	46	39.4
70	75	64	54.8
80	100	85	75

Table 2.3: Effect of indoor heating upon RH

Other Effects of Change in Moisture Content

The strength properties of the paperboard also changes with changes in the percent moisture content. The end to end (axial) crush strength increases with a decrease of moisture content. The side to side (flat) crush strength reaches maximum strength at about 5% moisture content but decrease as moisture content increase above 5%. According to CCTI [2], the axial crush strength and the flat crush strength decreased about 60% when percent moisture content changed from 7.5% to 14%.

Determining Moisture Content of Cores

The moisture content of a core can be measured by determining the difference between the dry weight of the core and the original weight of the core, then dividing by the original weight of the core. Because this change in weight is very small, a very

accurate scale is needed. CCTI [2] established a standard that the scale should be accurate to 0.1 percent of the specimens original weight.

Hakiel's Model

In order to produce a good quality wound roll, it is important to be able to predict the stress that develops within a wound roll. Knowing the stress helps determine the structural integrity of the web and helps predict efficient packaging of the roll. Z. Hakiel [7] has developed a model to help predict the stress in a center wound roll. Hakiel developed a second order differential equation which describes an incremental inter-layer pressure on the web. The differential equation can be solved numerically by a computer program. This paper will eventually use this model to help predict how moisture changes in the paperboard core effect the stress in the roll.

These assumptions were made about the web in Hakiel's model:

1. The winding roll is a geometrically perfect cylinder with the web having uniform width, thickness, and length.
2. The roll is a collection of concentric hoops. Winding is modeled by the addition of tensioned hoops. Roll properties remain constant.
3. The roll is an orthotropic, elastic cylinder with linear-elastic behavior in the circumferential direction and non-linear-elastic behavior in the radial direction. The radial modulus of elasticity is known and varies as a function of radial stress.
4. The stresses within the roll are a function of radial position only.

5. The roll is under a plane stress condition and axial stresses are equal to zero.

By combining equilibrium, compatibility, and constitutive expressions, Hakiel derived the following second order differential equation in radial pressure, σ_r:

$$r^2 \frac{d^2\sigma_r}{dr^2} + 3r\frac{d\sigma_r}{dr} - \left(g^2 - 1\right)\sigma_r = 0. \tag{2.1}$$

A variable δ is introduced. It represents the interlayer pressures developed at all layers due to the addition of this last layer of web accreted upon a winding roll which has an outside radius s. Equation (2.23) is rewritten as:

$$r^2 \frac{d^2(\delta P)}{dr^2} + 3r\frac{d(\delta P)}{dr} - \left(g^2 - 1\right)\delta P = 0. \tag{2.2}$$

Equation (2.2) is the governing equation in Hakiel's model. Two boundary conditions are necessary to solve this second order differential equation. The first condition is at the outside of the winding roll. It is found by assuming that the incremental interlayer pressure of the last lap is equal to the hoop stress of that lap:

$$(\delta \mathrm{P})\big|_{r_{last}} = \frac{T_w\big|_{r_{last}}}{s} b. \tag{2.3}$$

The second boundary condition occurs at the core and roll interface. The radial deflection of the core must equal that of the roll. The deflection at the core is given by the equation:

$$U(1) = -\frac{\delta P(1)}{E_c}. \tag{2.4}$$

[(1) represents the first layer of web.]

Using equilibrium, compatibility, and constitutive expressions equation (2.4) can be rewritten as:

$$\left.\frac{d(\delta P)}{dr}\right|_{r_i} = \left(\frac{E_t}{E_c} - 1 + \upsilon\right)\delta P\Big|_{r_i} . \tag{2.5}$$

Though the second order differential equation is linear, it is not possible to find an analytical solution to the problem. Since g^2 is not a constant but a function of inter-layer pressure, a numerical solution is sought in order to solve the boundary value problem. A finite difference method, using the central difference approximation for the derivatives, is employed to solve the differential equation. The central difference approximations are:

$$\left.\frac{d}{dr}(\delta P)\right|_{r_i} = \frac{\delta P_{i+1} - \delta P_{i-1}}{2h}, \tag{2.6}$$

$$\left.\frac{d^2}{dr^2}(\delta P)\right|_{r_i} = \frac{\delta P_{i+1} - 2\delta P_i + \delta P_{i-1}}{h^2} . \tag{2.7}$$

Substituting (2.7) and (2.6) into (2.2) and gathering terms yields the following:

$$\delta P_{i+1}\left(\frac{r_i^2}{h^2} + \frac{3r_i}{2h}\right) + \delta P_i\left(1 - \frac{2r_i^2}{h^2} - g^2\right) + \delta P_{i-1}\left(\frac{r_i^2}{h^2} - \frac{3r}{2h}\right) = 0 . \tag{2.8}$$

The first boundary condition is rewritten as:

$$\delta P_{i+1} = \frac{T_{i+1}}{r_{i+1}} h . \tag{2.9}$$

Using forward difference, the second boundary condition is:

$$\delta P_2 - \left[h\left(\frac{1}{h} + \frac{E_t}{E_c} - 1 + \upsilon\right)\right]\delta P_1 = 0 . \tag{2.10}$$

The equations (2.8), (2.9), and (2.10) can then be written in the matrix form:

$$[A]\{\delta\sigma\} = [B] \tag{2.11}$$

An iterative program steps through the roll adding one layer each iteration until the entire roll is analyzed; g^2 is recalculated for each iteration. The incremental stresses are then added together to obtain the total stress.

Thermal Analysis of a Wound Roll

Qualls [12] used Hakiel's model to calculate the inter-layer pressure in a wound roll subject to changes in temperature. The relevance to the present research is that Qualls modified Hakiel's model to account for the effects of thermal expansion of the core and web on the stresses within the roll. Whereas Quall's model accounted for core expansion due to temperature, it can be directly modified to account for expansion due to moisture content. The model added variables for the thermal expansion and contraction of a wound roll. The model is then solved similar to Hakiel's model. The governing second order differential equation becomes:

$$r^2 \frac{d^2\sigma_r}{dr^2} + 3r\frac{d\sigma_r}{dr} - \left(g^2 - 1\right)\sigma_r = E_t\left(\alpha_r - \alpha_t\right)\Delta T . \tag{2.12}$$

The core is also affected by thermal changes, therefore the inner boundary condition changes to:

$$\varepsilon_t = \frac{\sigma_r}{E_c} + \alpha_c \Delta T , \tag{2.13}$$

$$\varepsilon_t = \frac{1}{E_t}\sigma_t - \frac{\upsilon}{E_r}\sigma_r + \alpha_t \Delta T . \tag{2.14}$$

Combining equation (2.13) and (2.14) and solving like Hakiel gives the following:

$$r\frac{d\delta P_{r_1}}{dr} + \delta P_{r_1}\left(1 - \upsilon - \frac{E_t}{E_c}\right) = E_t\left(\alpha_c - \alpha_r\right)\Delta T . \tag{2.15}$$

The outer boundary condition assumes a traction free outer roll surface and zero stress.

$$(\delta P)\big|_{r=s} = 0 \tag{2.16}$$

The model is solved by first going through Hakiel's model and getting a stress distribution at the initial temperature. The temperature is then changed incrementally. A new inner boundary condition is calculated for the temperature change. A tri-diagonal set of simultaneous equations are then produced from equations (2.12), (2.15), and (2.16), the solution of which yields the pressure change within the roll due to the incremental

temperature change. The radial pressure and radial modulus are updated, and the process repeats itself until the required temperature change is achieved.

Viscoelastic Model of Paperboard Core

Henning [8] developed a viscoelastic model for a paperboard core. He showed that a core behaves linear viscoelastically and used Maxwell's model [4] to describe the behavior of his cores. Maxwell's model gave Henning a way to predict the strain in the core as a function of time and pressure. This strain was then used as a inner boundary condition for Hakiel's model. Using Hakiel's model the same way Qualls did, Henning was able to develop a model of how stress in a wound roll changes through time due to viscoelastic behavior of the core.

Henning started his model by doing a simple creep test to develop a creep compliance function for the core. The data gathered were fitted to the generalized creep function shown below.

$$J(t) = J_0 + J_1 e^{\frac{t}{T_1}} + J_2 e^{\frac{-t}{T_2}} \tag{2.17}$$

Henning determined J(t) for two core types at various constant external pressures. He discovered that J(t) could be normalized for both core types, by dividing the strain data by the applied pressure, thus giving evidence that both core types he tested were linear viscoelastic.

Knowing the creep compliance function, the following equation allowed Henning to determine the strain of the core from any stress input [4].

$$\varepsilon(t) = \int_0^t J(t-t') \frac{\partial \sigma(t')}{\partial t'} dt' \tag{2.18}$$

The equation (2.18) can be approximate as:

$$\varepsilon(t) = \sum_{n=1}^{n=j} J(t_n - t_{n-1})\sigma_n \tag{2.19}$$

Equation (2.19) gives the total strain of the core at any time t. Hakiel's model required incremental change. Therefore, the incremental change for equation 2.19 is

$$\varepsilon(\Delta t) = \left[J_0 + \sum_{i=1}^{2} J_i e^{\frac{-\Delta t}{T_i}} \right] \sigma_{r_1} \tag{2.20}$$

Adding this strain to the inner boundary condition yields the following:

$$r\frac{d\delta\sigma_{r_1}}{dr} + \delta\sigma_{r_1}\left(1 - \upsilon - \frac{E_t}{E_c}\right) = \left(J_0 + \sum_{i=1}^{2} J_i e^{\frac{-\Delta t}{T_i}}\right)\sigma_{r_1} \tag{2.21}$$

The outer boundary condition was the same as Qualls, σ_{rs}=0. The model was then solved by first running through Hakiel's model. This was done to produce an initial pressure profile for the roll. Maxwell's model of the core would then begin monitoring how the core deformed viscoelastically due to the interlayer pressure. The core deformation would then be updated and Quall's model would be solved to predict the reduced pressure. The new pressure would be used to predict the deformation for the next time step. A new pressure would be calculated, and the steps repeated.

Henning's model showed that the pressure change due to viscoelastic effect was localized to web material near the core, and that the pressure in the first layer of the web dropped to zero after 1500 minutes for the cores and webs used in his research.

CHAPTER 3

Radial Expansion Due to Change in Humidity

Initial Experiments

To gain insight on how a paperboard core changes dimensions due to a humidity change, an experiment was set up to observe how the core changes dimensions under different RH conditions. In the beginning, it was not obvious how best to achieve this. The first setup was to apply strain gauges to a core and let it go through a change in humidity. There was concern about how to fix the strain gauges to the core without affecting the core's ability to absorb water. Using epoxy or super glue would create a barrier that prevents water from entering the core at that point. It was finally decided to go ahead and attach strain gauges to a core, let it go through a humidity change, and compare the result to micrometer readings of the core diameter.

At the time this process was conceived, a control humidity chamber was not available; but since this was a test run to determine whether or not a strain gauge would work, only a change in humidity was necessary. A chamber was set up with water on the bottom and a stand on which the core was placed. The chamber is illustrated in Figure 3.1. The chamber was sealed, and RH readings were taken periodically. The chamber maintained a steady 85% to 90% RH. With the core initially at room condition of 42% to

45% RH, the chamber supplied enough moisture change so that a change in core dimensions was observed.

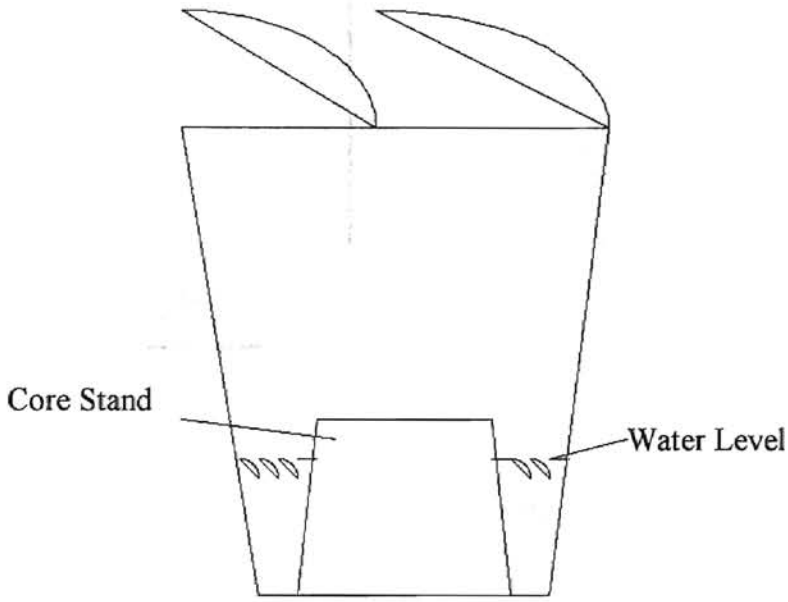

Figure 3.1: Temporary RH Chamber

It was decided that five strain gauges were to be positioned throughout the core. This was to see if the changes throughout the core were the same. The strain gauges were positioned through the core as shown:

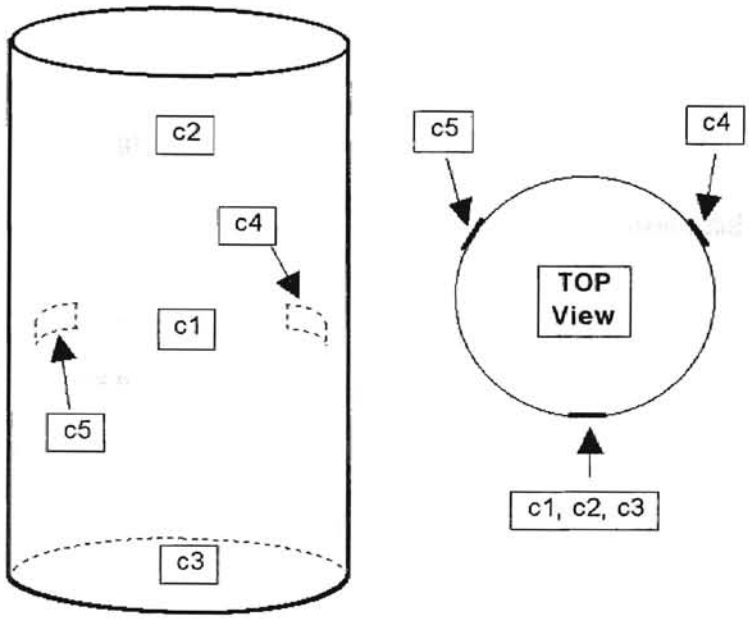

Figure 3.2: Position of Strain Gauges on First Test

Strain gauges c1, c4, and c5 were positioned circumferentially around the core. Gauges c1, c2, and c3 were positioned lengthwise along the core. Epoxy was used to glue the strain gauges to the core. The gauges were connected to a switch and balance box, which was connected to a strain indicator box. The switch and balance box was needed because the strain indicator could not be connected to all the gauges, simultaneously.

The strain gauges used were Measurements Group model CEA-06-240UZ-120. This type of strain gauge was used because it was readily available and inexpensive. The core strain was to be measured at constant temperature, so the strain gauge comfortably met the needs of the experiment. The strain indicator was Measurements Group 3800 wide range strain indicator. The switch and balance box was made by Budd Instrument model SB-1. The switch and balance box and strain gauge indicator combination were checked for accuracy by testing the strain on a cantilever beam. The strain equation for a cantilever beam is:

$$\varepsilon = \frac{3Wc}{L^2} \tag{3.1}$$

For a beam of .5 inch width, 1/8 inch thick, and 10 inches long, the strain was calculated to be 1875 micro-strain. The strain reading from the cantilever beam read 1845 micro-strain.

After the strain gauges were applied to the core, a micrometer was used to measure the diameter of the core. Specific points were labeled on the core so that the same point could be measured after the dimensions changed. The strain gauges were then connected to the indicator and put into the temporary environmental chamber. Readings were taken periodically. The results are shown below:

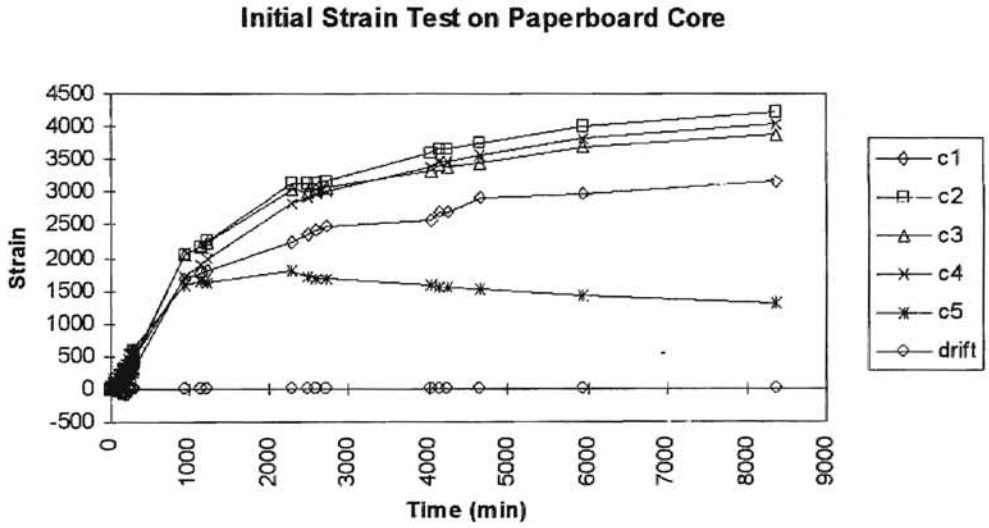

Figure 3.3: Initial Core Test

The drift line is the reading from a strain gauge glued to an aluminum plate to test for drift in the system. The test was run for six days and showed that most of the change occurred within the first two days of the experiment. After the six days were up, the core diameter

was measured again at the same points at which they were labeled. Results are shown below:

	Before			
	Top (c2)	Middle (c1)	Middle (c5)	Bottom (c3)
	3.4068	3.407	3.409	3.4077
	3.408	3.4077	3.409	3.4077
	3.407	3.4087	3.41	3.4071
	3.4065	3.4078	3.4085	3.4066
Average	3.4071	3.4078	3.4091	3.4073

Table 3.1: Diameter of core at room condition

	After			
	Top (c2)	Middle (c1)	Middle (c5)	Bottom (c3)
	3.4448	3.4386	3.4562	3.4416
	3.4463	3.4376	3.4545	3.4437
	3.444	3.44	3.4552	3.4423
	3.4438	3.4384	3.4542	3.4431
Average	3.4447	3.4387	3.4550	3.4427

Table 3.2: Diameter of core after taking out of environmental chamber

	Strain			
	Top (c2)	Middle (c1)	Middle (c5)	Bottom (c3)
	0.01105	0.00905	0.01346	0.01039
Average	0.01099			

Table 3.3: Strain result from before and after data

The 11,000 micro-strain result from the micrometer is significantly higher than the strain gauges reading 4000 micro-strain. Since the tangential strain of a cylinder is defined as u/r, the two readings should be similar. Because the two readings are not similar, the result showed that the epoxy significantly affected the response of the core to the moisture change. The result of the micrometer tests are deemed correct as the test was a measure of the primary variable, the change in diameter due to change in moisture content, and because use of the micrometer in no way impeded moisture transferring into the core. The strain gage measurements were questionable since they locally impeded moisture, and repeatability was questionable. Thus, an alternative means of measuring the diametral changes was investigated.

DCDT Measurement

The result from the first test showed that the best way to attack the problem is to measure the radial change by some sort of physical contact method. Since the test would go on for 2 days, it was also desired that the method of measurement be electrical so that a data acquisition board could be used to record the data. An obvious choice for this type of measurement is a direct current differential transformer (DCDT). From the experimental results above, the DCDT needs to have a linear range of .05 inch. Three Trans-Tek DCDT model # 0200-0001 were acquired to measure the core diameter

changes. The working range of the DCDT was ± .05 inches. The input voltage could range from 5 to 7 volts, but the recommended and tested voltage was 6 volts. Each DCDT was individually calibrated at the factory. The voltage-to-displacement constants are listed below.

DCDT	VDC/Inch/Volt Input
A	5.5969
B	5.5976
C	5.7213

Table 3.4: Voltage to Displacement Constant

A fixture was designed to hold the DCDT and the core. Figure 3.4 shows a sketch of the fixture. The fixture is made of two aluminum plates, connected by four steel rods. The two steel rods on the bottom are used to hold the core. The aluminum cube that runs along the top two steel rods is used to hold the DCDT. The DCDT is held in place by set screws. The DCDT displacement rods are held in contact with the core by gravity.

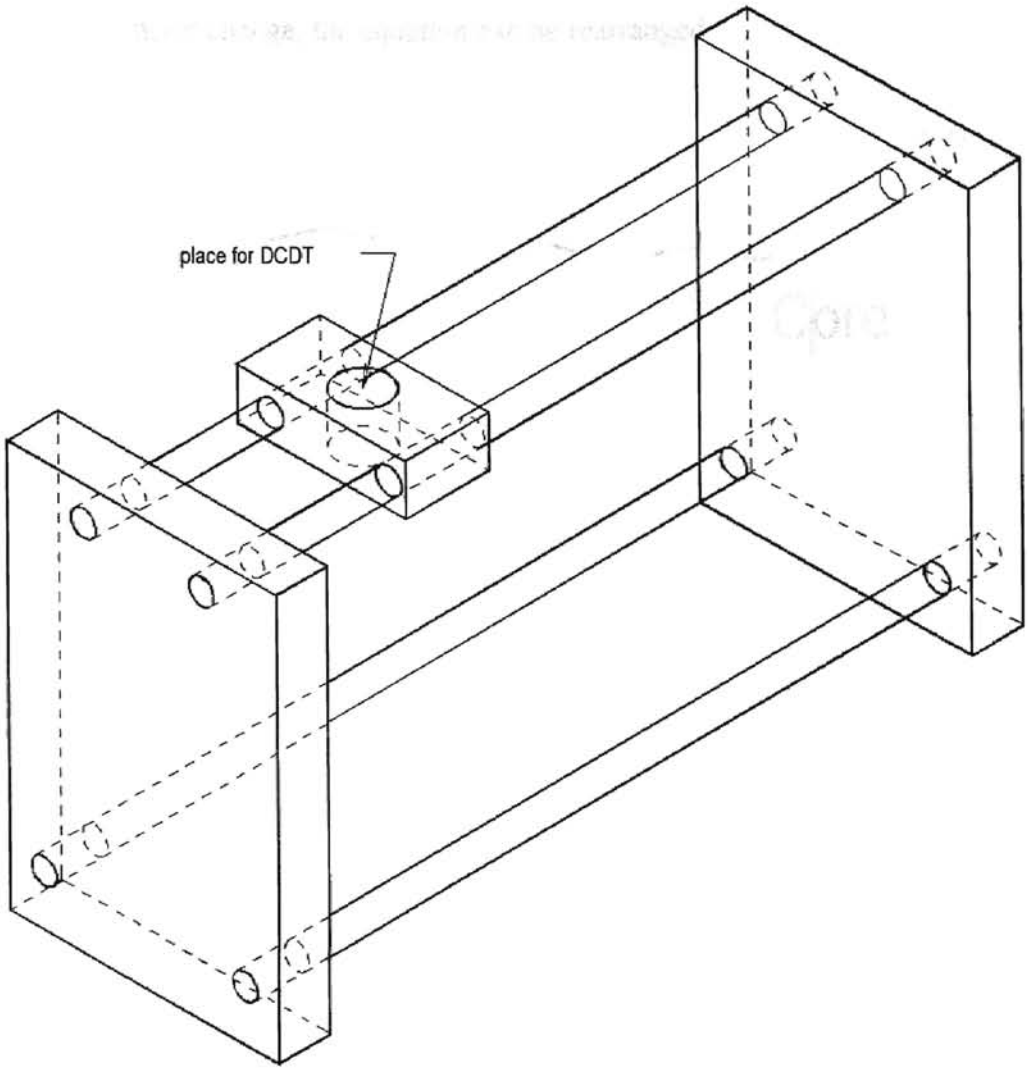

Figure 3.4: DCDT housing

Because of the way the core sits within the fixture, the DCDT does not directly measure the radial displacement. The DCDT displacement reading is a function of the geometry. As Figure 3.5 shows, the DCDT output can be described by the following equation:

$$\frac{\Delta D}{2} + \frac{\Delta D}{2}\cos\theta = \Delta(\text{DCDT}) \ . \qquad (3.2)$$

Solving for diameter change, the equation can be rearranged:

$$\Delta D = \Delta(\mathrm{DCDT})\left(\frac{2}{1+\cos\theta}\right). \tag{3.3}$$

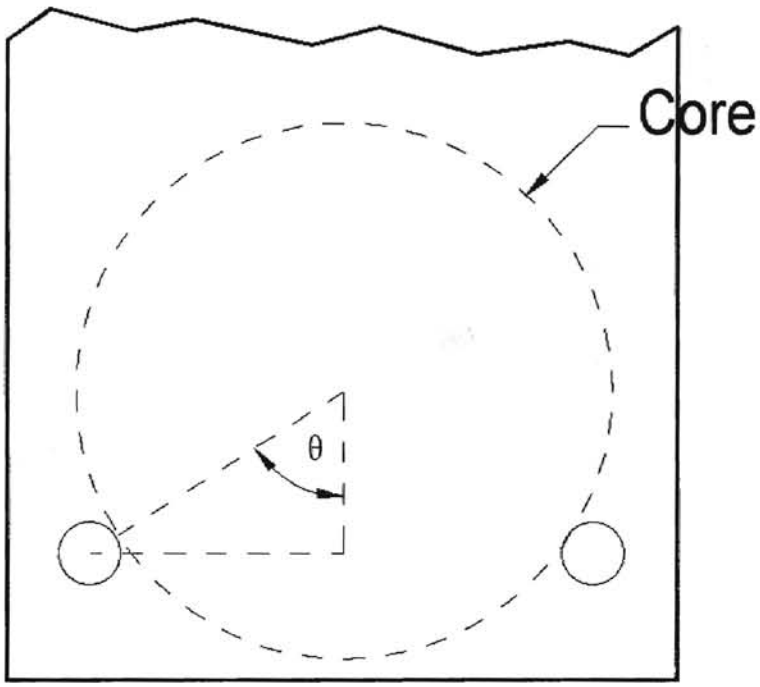

Figure 3.5: Side View of core resting on DCDT housing

Power was supplied to the DCDT by the BK Precision triple output DC power box, model 1660. Voltage output was adjusted so that six volts would be supplied to the DCDT.

Brass Shim

It is known that a core loses strength as it gains moisture [2]. This affects the core modulus (E_c), which is an integral part of determining stress in a wound roll. Therefore, a fixture that allows for the monitoring of the pressure that the core can exert, as a function of hygroscopic expansion, needed to be developed. The problem was solved by tightly

wrapping a brass shim stock around the core and strain-gauging the shim, as described below. The shims used were .002 inch thick and a half-inch wide.

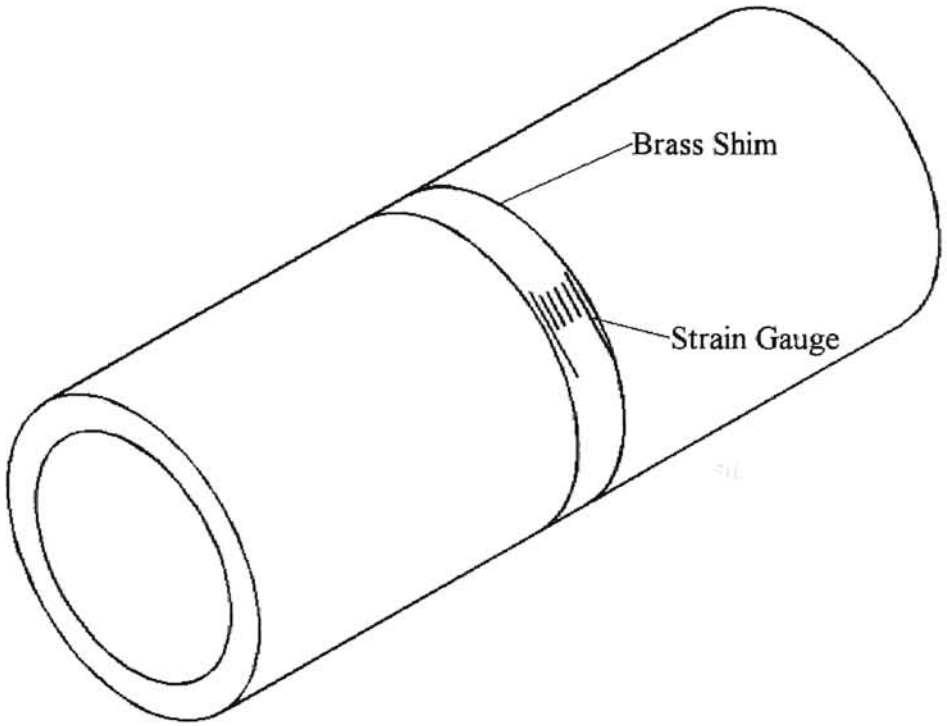

Figure 3.6: Brass shim wrapped around core

One end of the shim was glued to the core. The shim was then wrapped around the core, overlapping itself by an inch and glued to the overlapping bras shim. The adhesive used to glue the brass strip down was super glue. A figure of this is shown in Figure 3.7. To ensure that the brass shim had a consistent pre-stress before testing, 1.25 lb or a 2.5 lb weight was hung off the brass shim while it was being wrapped around the core.

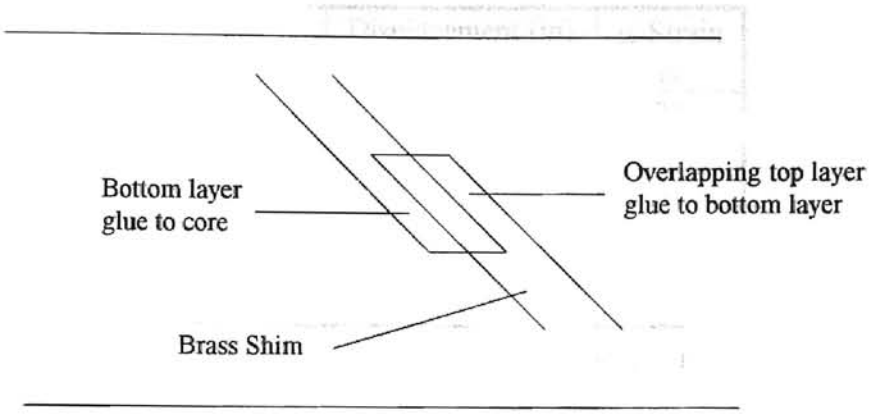

Figure 3.7: Gluing brass shim to core

Data Acquisition Board

Data was collected by a Metrabyte Dash-16F data acquisition board. The Dash 16F board is a 12 bit board. The voltage input has the ranges of +1v, +2v, +5v, +10v unipolar and ± 0.5v, ± 1v, ± 2.5v, ± 5v, ± 10v bipolar which can be manually set on the board. For the experiment, the board was set to collect data from +/- 5 volts. The program used to store and save the data was Labtech Notebook. Labtech Notebook is a menu driven data acquisition program written by Laboratory Technologies Corporation. Because the board is 12 bits, the accuracy of the board voltage reading is .00244 volt. The voltage reading is directly proportional to the displacement reading of the DCDT. Table 3.5 shows the minimum displacement and strain readings each DCDT can monitor in this setup.

DCDT	Displacement (in)	μ-Strain ε_t
A	$7.26e^{-5}$	21
B	$7.26\ e^{-5}$	21
C	$7.11\ e^{-5}$	21

Table 3.5: Minimum accuracy of DCDT

Note that the strains reading were determined using 3.41 inches as the initial length. This is the average outside diameter of the cores that are going to be measured.

Testing Procedure

The DCDT housing was placed in an environmental chamber that could control both temperature and RH. The environmental chamber was made by Standard Environmental System Inc., model RTT/6S. The DCDT wiring was ported out of the environmental chamber via a hole at the bottom of the chamber. The output from the DCDT was connected to the DASH-16 data acquisition board and the input was connected to the DC power supply.

An eighteen inch long core was cut into three equal sections of six inches. One section (designated core section C1) was wrapped by brass shim stock and strain gauged. When testing first began, only one brass shim stock was wrapped around the core, later tests had two brass shims wrapped around the core. This was because in the early experiments there was more concern with the core expansion than the core E_c changes. Later, two shims were installed to see if similar E_c readings could be obtained. The core initial diameter was recorded with a micrometer. This was done at nine locations along the length of the core, to obtain an average measurement. The core section was then put

into the DCDT housing. Two DCDTs were placed an inch from each end, and one in the middle of the core. A DCDT was always on a brass shim (When two brass shims were used only one DCDT was recording the free expansion of the core. The other two recorded the constrained expansion of the core due to the brass shim). The data of how the core changed due to constraint of the brass shim were needed to calculate E_c. Wires from the strain gauge would be ported out to the strain indicator and data acquisition board. A second core section (this section is C2) was then put in the environmental chamber for measuring moisture content purposes.

After everything was set up, the following procedures were followed:

1. The two cores were left in the chamber for two days at 45% RH and 75°F. This was done to ensure that the core was at equilibrium at 45% RH before tests were performed on the core.
2. At the end of the two days, core C2 was weighed by a Satorius scale model 1712 MP8. (The scale is accurate up to .0001 gram and can measure up to 160 grams. Since the core weight can range from 120 to 150 grams, the scale more than qualified for the precision needed to meet the standard set by CCTI [6].)
3. Core C2 was placed back in the environmental chamber. The RH of the chamber was then increased to 60 percent, and the data acquisition program was started.
4. After two days had passed, steps two and three were repeated for 75% and 90% RH.

The test was run on the same two sections of core for 45% to 60% RH, 60% to 75% RH, and 75% to 90% RH.

Core Expansion Data Analysis

The data collected from the DCDT were in voltage form. Using the sensitivity constants above, the voltages were transformed into displacement and divided by the initial diameter to attain strain data. The data presented below are the average of 8 tests that were done.

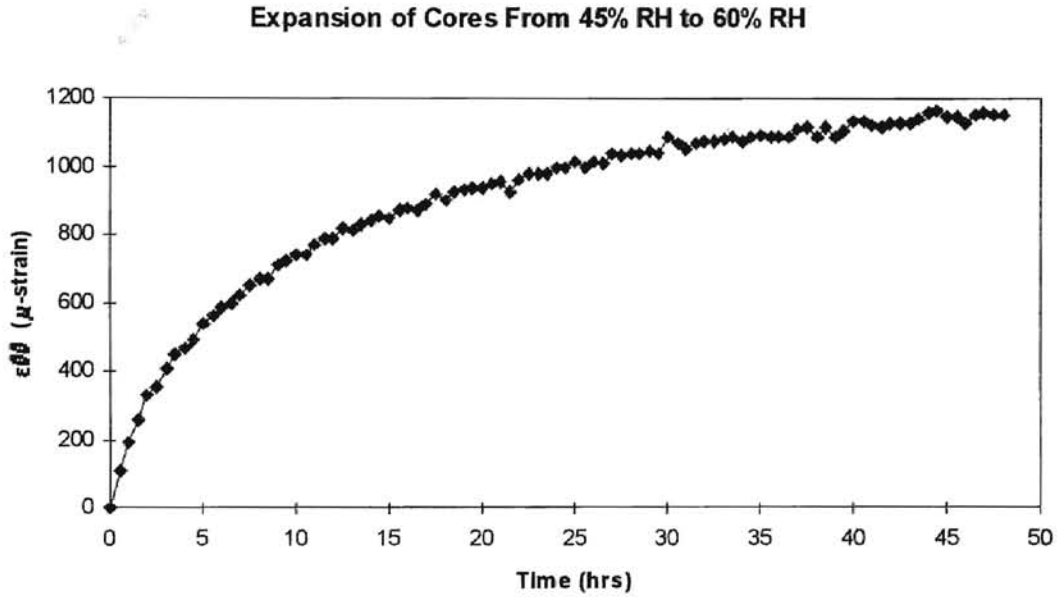

Figure 3.8: Expansion Data of Cores from 45% to 60% RH

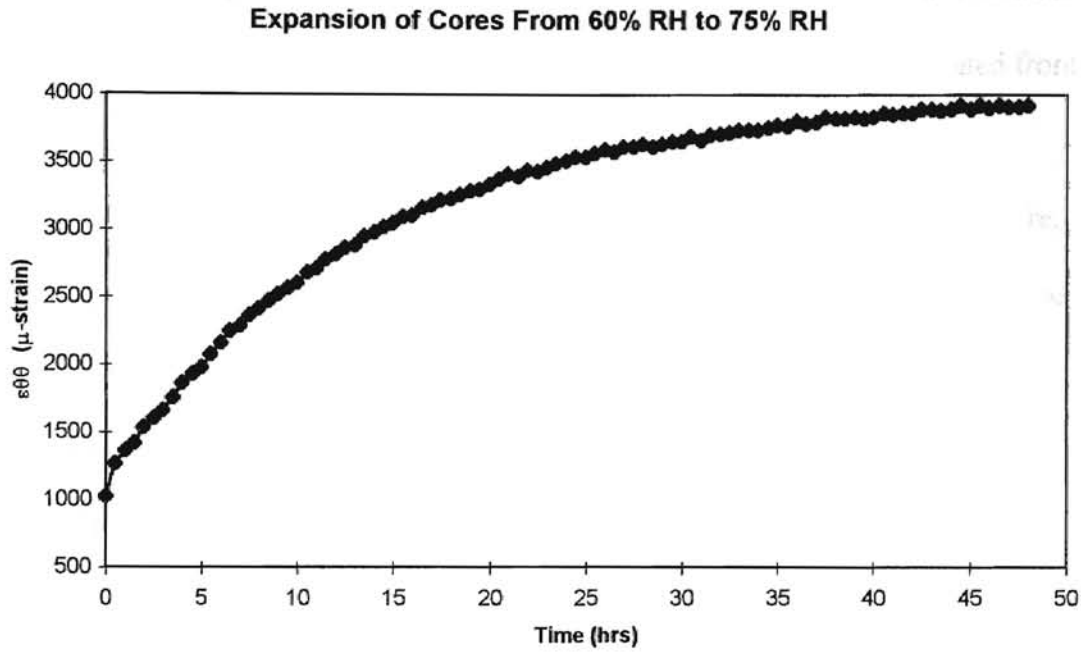

Figure 3.9: Expansion Data of Cores from 60% to 75% RH

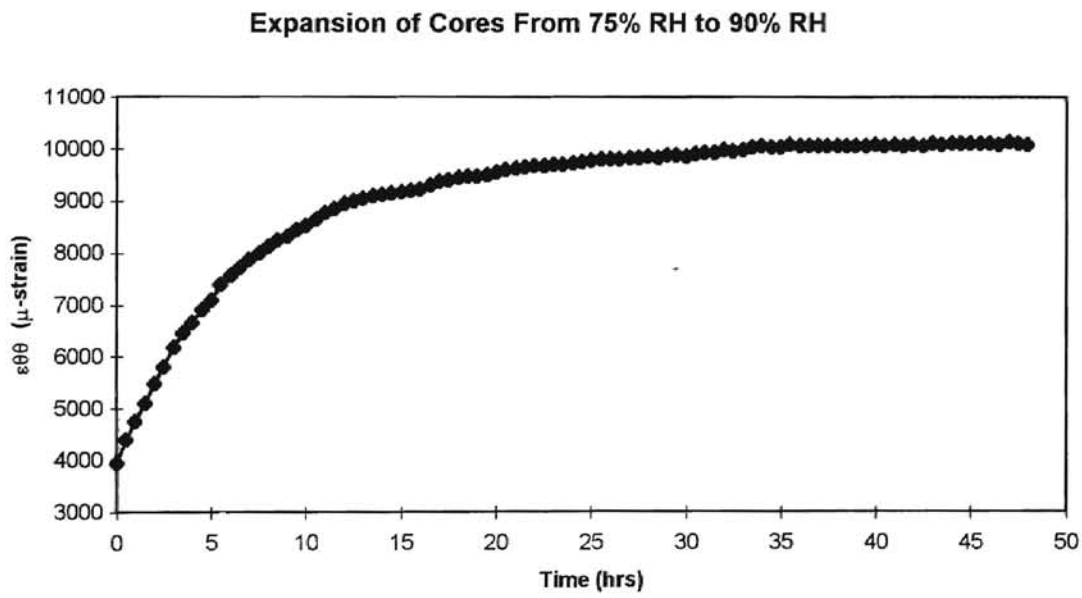

Figure 3.10: Expansion Data of Cores from 75% to 90% RH

The reason the strain in Figure 3.9 and Figure 3.10 do not start at zero strain is because they show a continuous strain from 45% RH. All strains were calculated from the initial diameter measurement.

Table 3.3 and Figure 3.10 showed that as long as the core is gaining moisture, the course the core takes from start to final humidity condition does not matter, as long as it goes through the same RH change, it will reach the same final condition. Table 3.3 showed a core going through a step change from 45% RH to 90% RH. Figure 3.10 showed a core starting at 45% RH step changing to 60% RH, 75% RH, and 90% RH. Even though both cores took different course to reach 90% RH, they both showed a similar change in strain. Table 3.3 and Figure 3.10, also, showed two methods of measuring strain that gave similar results. The results gave confidence that the DCDT data were measuring what was occurring.

To show how much strain occurred during each test, the initial strains at time zero were null and a composite plot is shown in Figure 3.11.

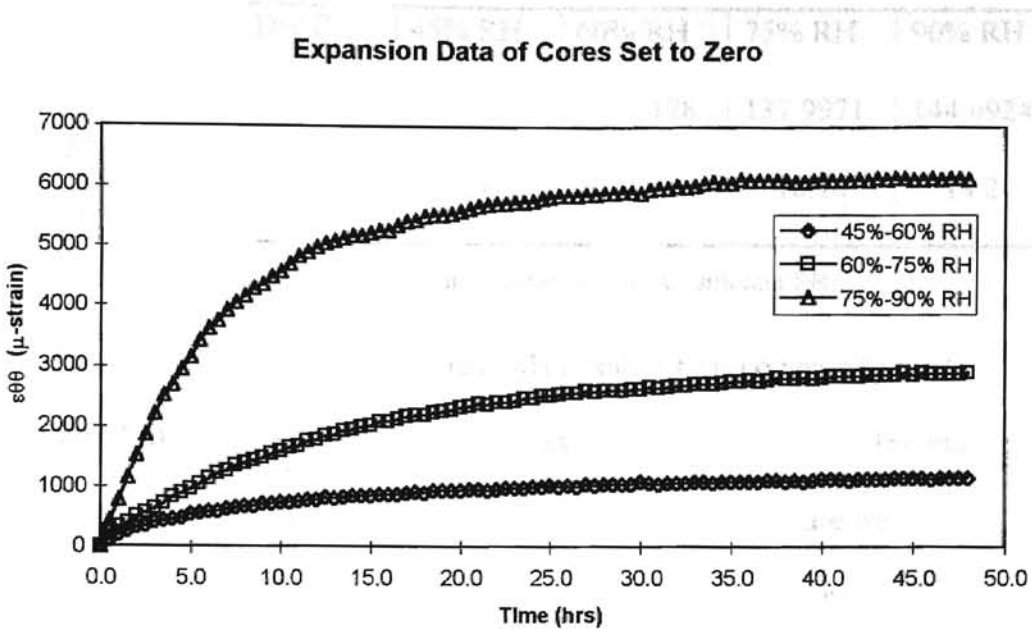

Figure 3.11 Expansion of Core Set to Zero

The curve shows that at high humidity the core expands a lot more for a given RH difference. It was desired to somehow relate these curves to the RH change. The CCTI [2] indicated that we can relate the dimension change of a paperboard core to the percent moisture of the core. With this information, the weight of the core was use to determine percent moisture content of the core. Percent moisture content can be computed by:

$$\% \text{ Moisture Content} = \frac{\text{Wt}_{\text{orginal}} - \text{Wt}_{\text{dry}}}{\text{Wt}_{\text{original}}} \times 100 \qquad (3.4)$$

The table below lists the average weight of the core and corresponding percent moisture content of the core from eight tests.

	Dry Core	45% RH	60% RH	75% RH	90% RH
Ave. Weight (gram)	123.9423	134.0943	135.3178	137.9971	144.4924
% Moisture Content	0.0	7.57	8.41	10.18	14.22

Table 3.6: Percent Moisture of Core at Different RH

When the percent moisture content versus RH (Table 3.6) is compare to the CCTI [2] data (Table 2.2), the data from Table 3.6 correspond well with CCTI. The maximum deviation occurs at 90% RH, 1.8% off. The other RH conditions are within .5% off. The free expansion of the core can also be compare to CCTI. For each percentage unit change in moisture content of the core, CCTI predicted a .09% change (designated N1) in the core outside diameter. This research calculated the N1 change to range from .14% to .17%, depending on which free expansion data were used to calculate N1 (refer to Table 3.7). CCTI never reported the type of paperboard they used for the test, only that N1 is a "rule of thumb" to predict the dimension of the core. Therefore, the discrepancy between the data could be due to different core type.

	$\frac{\Delta D}{D}$ / % change in moisture content
CCTI	.09%
45% RH to 60% RH	.14%
60% RH to 75% RH	.17%
75% RH to 90% RH	.15%

Table 3.7: Dimension Change of Recorded Data Compare to CCTI

When the data from Figure 3.11 were divided by the change in percent moisture content of the core, the following normalized data were produced. (Note that the percent

moisture changes from: 45% RH to 60% RH is .84%; 60% RH to 75% RH is 1.77%; 75% RH to 90% RH is 4.04%.)

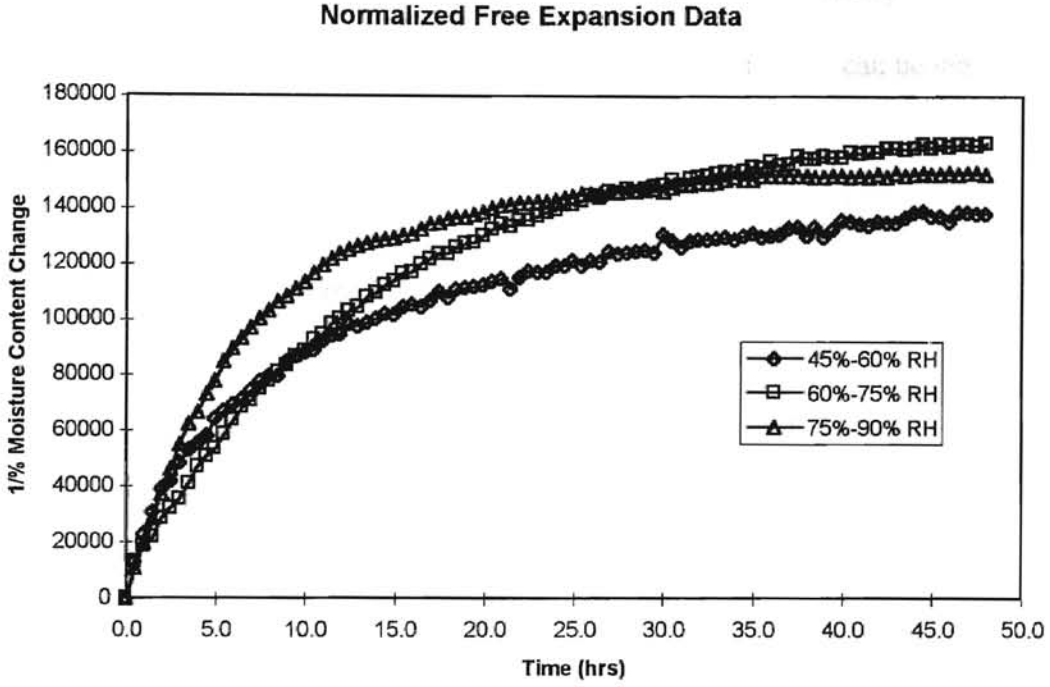

Figure 3.12: Normalized Expansion Data

The graph shows that all data converge when divided by the percent moisture change of the core. This can be verified by taking the equilibrium point from Figure 3.9 and 3.10 and dividing it by percent moisture change from 45% RH.

Equilibrium Point	3900 (60%-75% RH)	10000 (75%-90% RH)
% Moisture Change from 45% RH	2.61	6.65
Normalize Change	149000	150000

Table 3.8: Normalized Calculation for 45%-75% RH and 45%-90% RH

The data in Figure 3.12 allow for the prediction of the core circumferencial strain by knowing the percent moisture change of the core. By averaging the data in Figure 3.12 and fitting a polynomial through it, the strain rate of a core can be determined by multiplying the polynomial by any step change in percent moisture change. The polynomial is named humidity compliance function H(t). Strain rate can be determined by:

$$\varepsilon(t) = \frac{\chi}{100} H(t) \qquad (3.5)$$

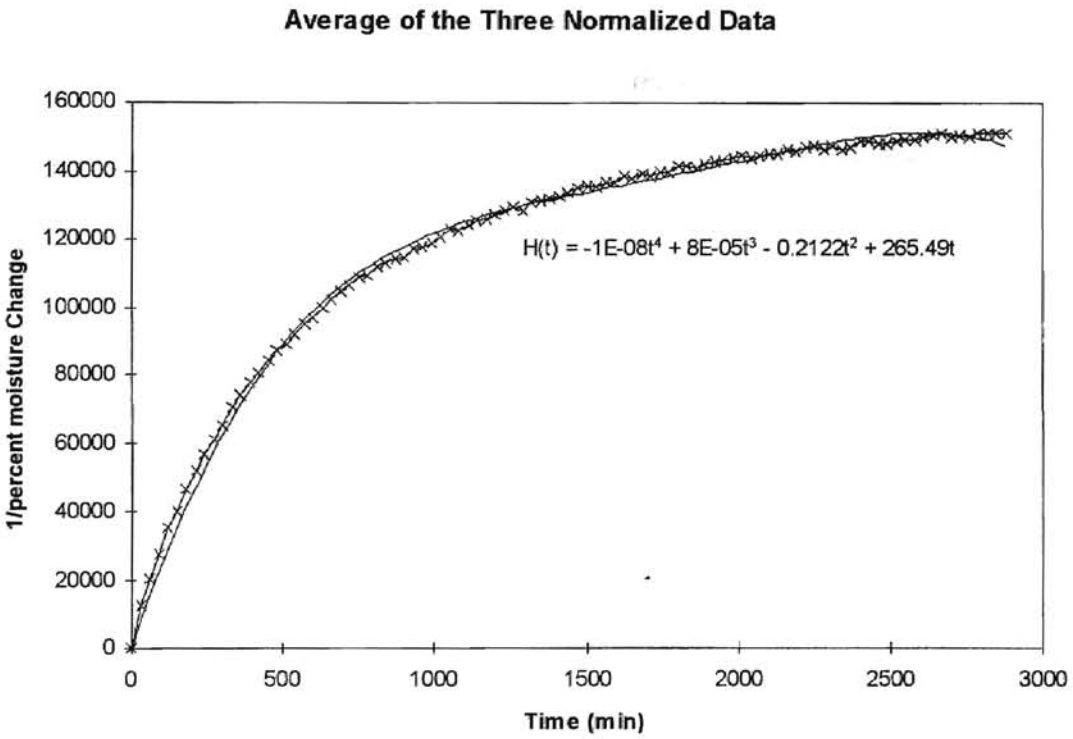

Figure 3.13: Normalized Humidity Data

Figure 3.13 shows the average data from Figure 3.12 with a fourth order polynomial fitted through the average points. The polynomial is the humidity compliance function for the type of core tested. Note that H(t) should always start at zero, to represent that there is no strain at time zero.

$$H(t) = -1(10^{-8})t^4 + 8(10^{-5})t^3 - .2122t^2 + 265.49t \qquad (3.6)$$

E_c Using Brass Shim Transducers

Brass shim(s) wrapped around the core were used to calculate the core modulus. The theory behind this was to model the part restricted by the brass shim as a press fit on a thick wall shell. The DCDT data on the unrestrained part of the core were used as the original diameter of the core. The DCDT data restrained by the brass shim were used as the press fit diameter of the core and brass shim. The strain reading from the strain gauge on the shim was used to calculate pressure between the shim and the core.

The pressure between core and shim was calculated using the thin wall pressure vessel expression:

$$P = \frac{\sigma_t c_{brass}}{r_{out}} = \frac{E_{brass}\varepsilon_{brass}c_{brass}}{r_{out}} = \frac{30800\varepsilon_{brass}}{r_{out}} \qquad (3.7)$$

The radial deformation inward can be obtained from DCDT data:

$$D_i = \left(\varepsilon_{DCDTu} - \varepsilon_{DCDTr}\right)r_{out} \qquad (3.8)$$

The elastic modulus of the paperboard material can be obtained from the press fit equation.

$$E_{cm} = \frac{Pr_c}{D_i}\left[\frac{r_{out}^2 + r_{in}^2}{r_{out}^2 - r_{in}^2} - \upsilon_c\right] \qquad (3.9)$$

The core modulus was calculated from the core material and geometry [15]:

$$E_c = E_{cm}\left[\frac{r_{out}^2 - r_{in}^2}{r_{out}^2 + r_{in}^2 - \upsilon_c\left(r_{out}^2 - r_{in}^2\right)}\right] \qquad (3.10)$$

The eight tests were averaged, and the following E_c were calculated from the data.

average (1.25 lb strap)							
RH%	εbrass(μS)	εθθ,DCDTr(μS)	εθθ,DCDTu(μS)	P(psi)	Di (in)	E_{cm}	E_c
60	350	700	1100	6.33	0.000681	1.42E+05	1.58E+04
75	1050	2100	4000	19.0	0.003239	8.97E+04	9.98E+03
90	1200	4800	10000	21.6	0.008889	3.75E+04	4.16E+03

average (2.5 lb strap)							
RH%	εbrass(μS)	εθθ,DCDTr(μS)	εθθ,DCDTu(μS)	P(psi)	Di (in)	E_{cm}	E_c
60	250	650	1100	4.52	0.000766	9.02E+04	1.01E+04
75	800	2200	4000	14.5	0.003069	7.22E+04	8.03E+03
90	1100	5200	10000	19.8	0.008208	3.72E+04	4.13E+03

Table 3.9: E_c Calculation from Brass Shim Data

The core elastic modulus calculated from this test was low when compare to with tests performed in the next chapter. There are many reasons possible. Probably the main reason is that this test does not take into account viscoelastic effects. The data does show E_c decreasing with increased moisture content. CCTI [6] claimed that axial and side to side strength decreased with increase in moisture content, and so a decrease in E_c might seem reasonable. However strength and modulus properties are entirely different entities, and no references state that modulus is effected by moisture content. This will be discussed further in Chapter 4.

CHAPTER 4

Viscoelastic Tests

Previous Viscoelastic Tests for Paperboard Core

The procedures for testing the viscoelastic properties of a core were develop by Jeff Henning. The same procedures were use to test cores for this research. His fixture was designed to perform a simple creep test. A steady state pressure was applied to the core and the circumferential strain was measured through time. To achieve this, Henning designed a pressure vessel that applied pressure to the outside of the core, while venting the inside of the core to the atmosphere. This effectively simulated the pressure on the core which was exerted by the wound on web. The strain data were collected by strain gauges glued onto the core. Detail on the pressure vessel and it supporting instrumentation were presented in Henning's thesis [8].

Testing Procedures

A 18 inch core was cut to 14 inches (this was done to be consistence with Henning's core length). The core was then placed in the environmental chamber for two days to equalize at a certain humidity. After two days, the core was taken out of the chamber and fitted with strain gauges. The core end caps were press fitted. The core outside was then wrapped with 3M poly tape. This was done in order to prevent air

leakage through the core itself. This was very important in this test. Because, any leakage through the core would change the moisture content of the core, therefore invalidating the test. When wrapping the tape around the core, special care was needed to ensure no wrinkles formed in the tape. Any wrinkle could cause a leak. A plastic bag wrapped around the core and the shaft added another barrier to prevent air from leaking through the core.

Wiring from the strain gauge was ported to the strain indicator via a bulkhead. The data acquisition program was started, taking data at 2 hertz. A pressure of 50 psi was applied to the chamber and data were obtained for four minutes. This procedure was to acquire data in the elastic region of the core. Once the four minutes was up, the data acquisition was reconfigured to take data every 5 minutes for a day. The data acquired here was used to determine the viscoelastic properties of the core. These procedures were done for cores which had been saturated at 45%, 60%, 75%, and 90% RH.

Viscoelastic Properties of Core at Different Humidities

The general purpose of the viscoelastic test is to gather data to produce the creep compliance function J(t). In order to get strain unit from equation (2.18), the J(t) function has to have the unit strain/psi (or 1/psi). The general form of the J(t) function is:

$$J(t) = J_0 + J_1 e^{\frac{-t}{\tau_1}} + J_2 e^{\frac{-t}{\tau_2}} \qquad (4.1)$$

(Additional exponential terms are sometimes required to fit the data)

In order to make unit of the collected data resemble the creep compliance function, the collected strain data were divided by the applied stress. The following figures show the strain data and the associated creep compliance functions for each RH conditions tested.

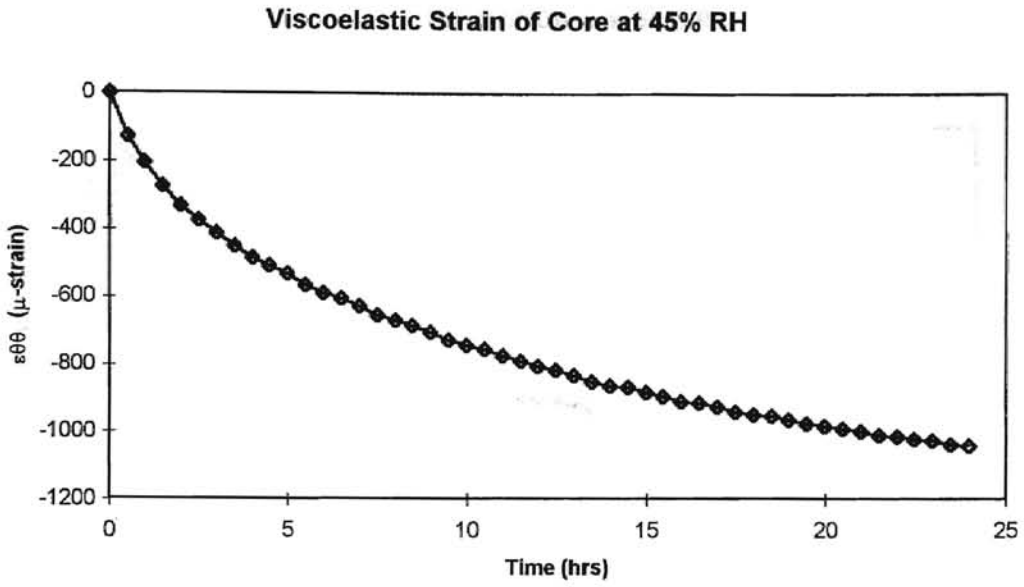

Figure 4.1: Viscoelastic Strain at 45% RH

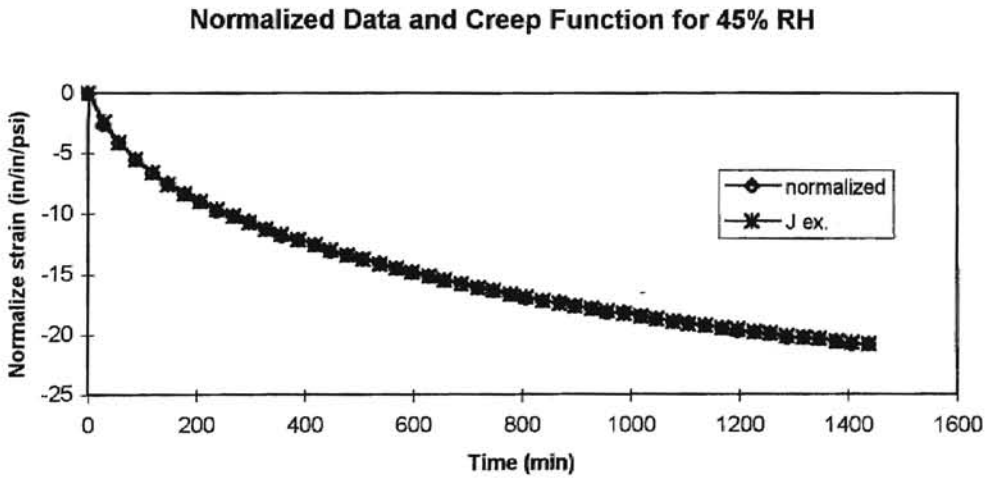

Figure 4.2: Creep Compliance at 45% RH

Creep compliance for 45% RH:

$$J(t) = -24.38 + 5.16e^{\frac{-t}{76.75}} + 19.22e^{\frac{-t}{856.32}} \qquad (\mathrm{J}(\mu\varepsilon),\ \mathrm{t(min.)} \qquad (4.2)$$

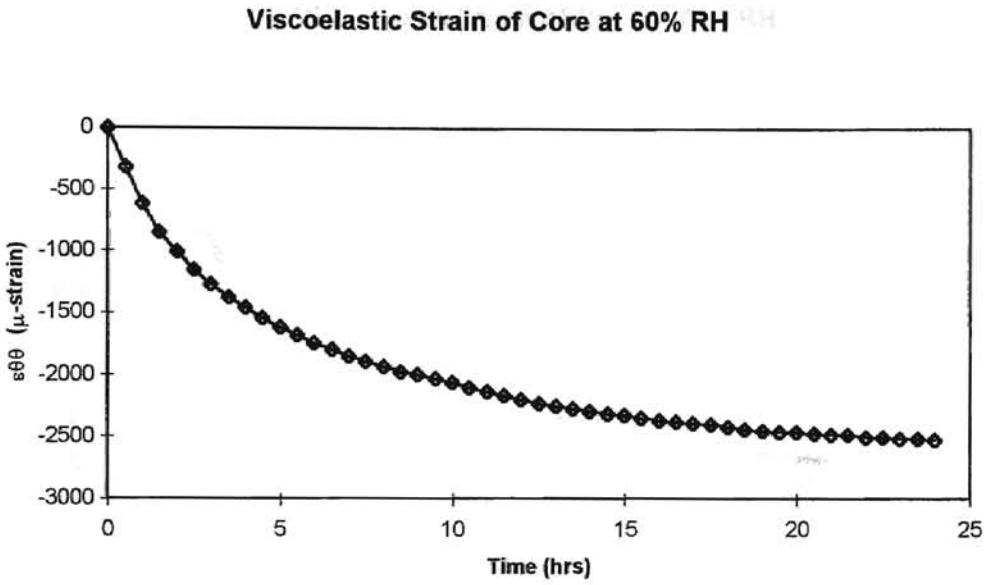

Figure 4.3: Viscoelastic Strain at 60% RH

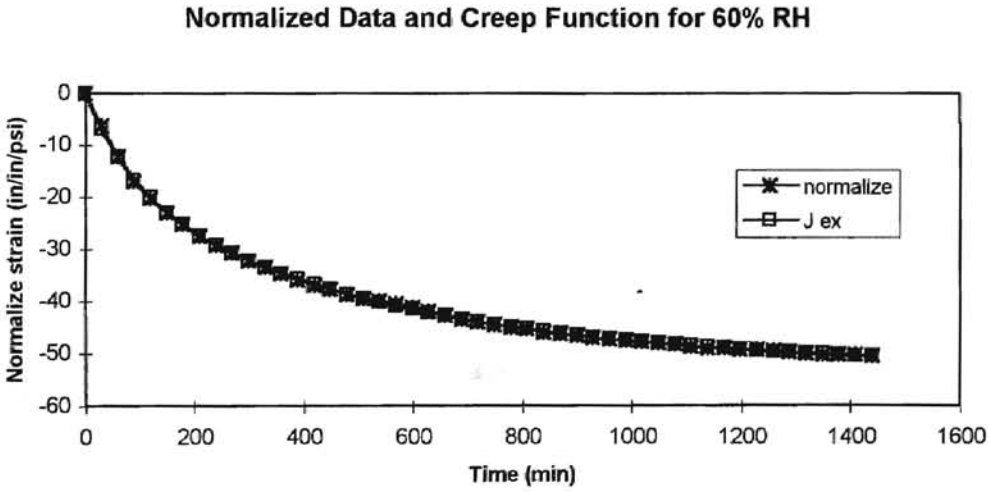

Figure 4.4: Creep Compliance at 60% RH

Creep compliance for 60% RH:

$$J(t) = -52.67 + 16.74e^{\frac{-t}{86.28}} + 35.92e^{\frac{-t}{505.65}} \qquad \text{(J(με), t(min.)} \qquad (4.3)$$

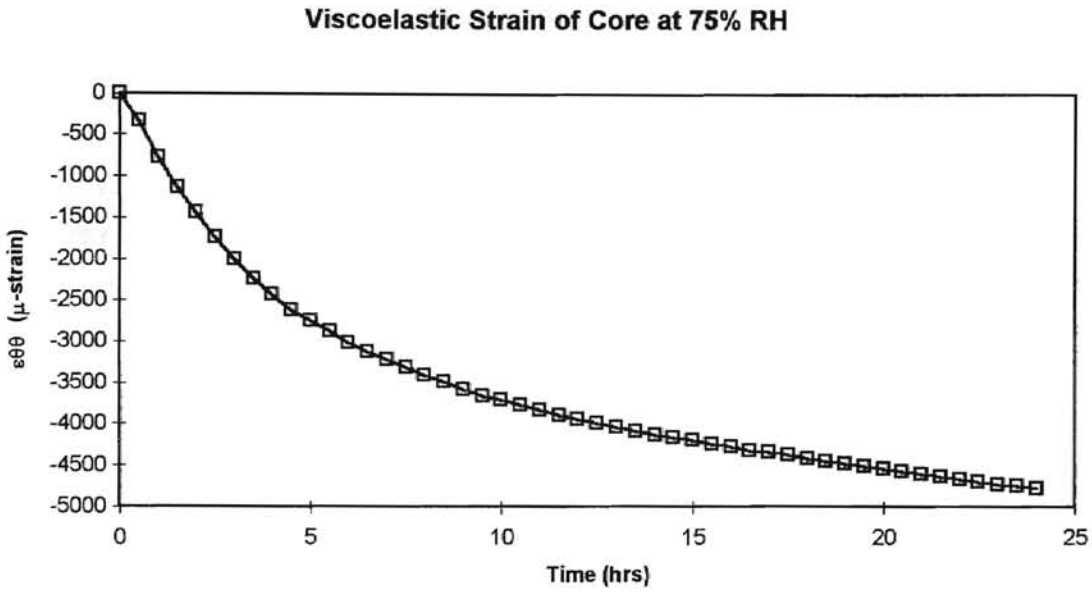

Figure 4.5: Viscoelastic Strain at 75% RH

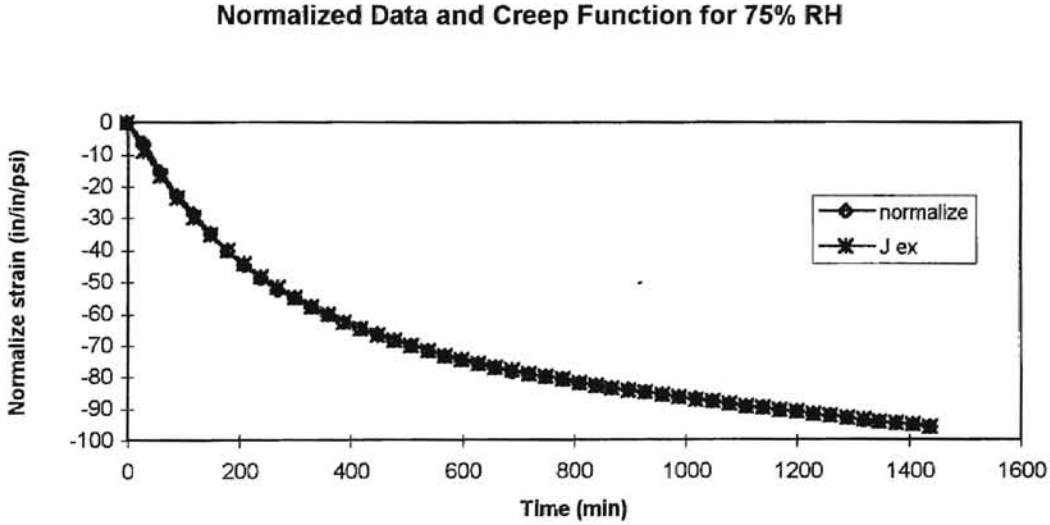

Figure 4.6: Creep Compliance at 75% RH

Creep compliance for 75% RH:

$$J(t) = -172.90 + 64.53e^{\frac{-t}{225.71}} + 108.37e^{\frac{-t}{4220.07}} \qquad \text{(J(με), t(min.)} \qquad (4.4)$$

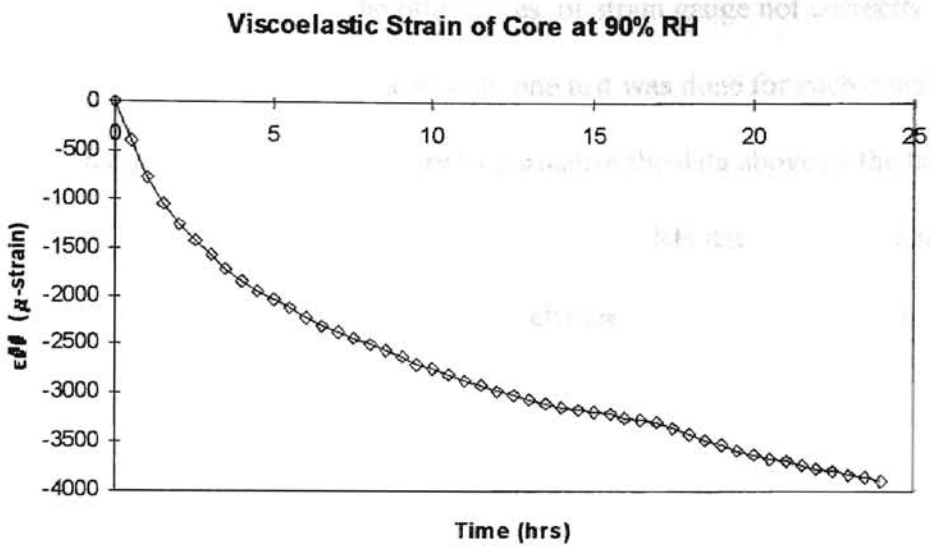

Figure 4.7: Viscoelastic Strain at 90% RH

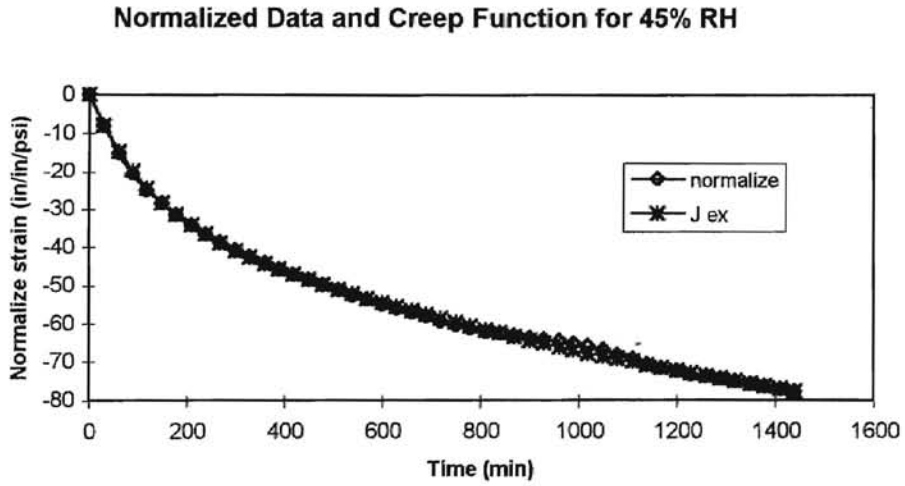

Figure 4.8: Creep Compliance at 90% RH

Creep compliance for 90% RH:

$$J(t) = -108.6 + 28.79e^{\frac{-t}{115.93}} + 79.81e^{\frac{-t}{1516.6}} \qquad \text{(J(με), t(min.)} \qquad (4.5)$$

The data shows that as the humidity increased strain due to viscoelastic effect also increased, except for 90% RH. The variation at 90% RH can be due to the core not

having the same properties as the other cores, or strain gauge not correctly connected to the core. Because of time constraint, only one test was done for each condition.

An effort was also made to try to normalize the data above to the humidity change. Some convergence was seen when the 60% and 75% RH data were divided by the percent moisture content change when the humidity changed from 45% to 60% and from 60% to 75% respectively. However, the data is not conclusive enough to conclude that convergence occurs when it is divided by the percent moisture change.

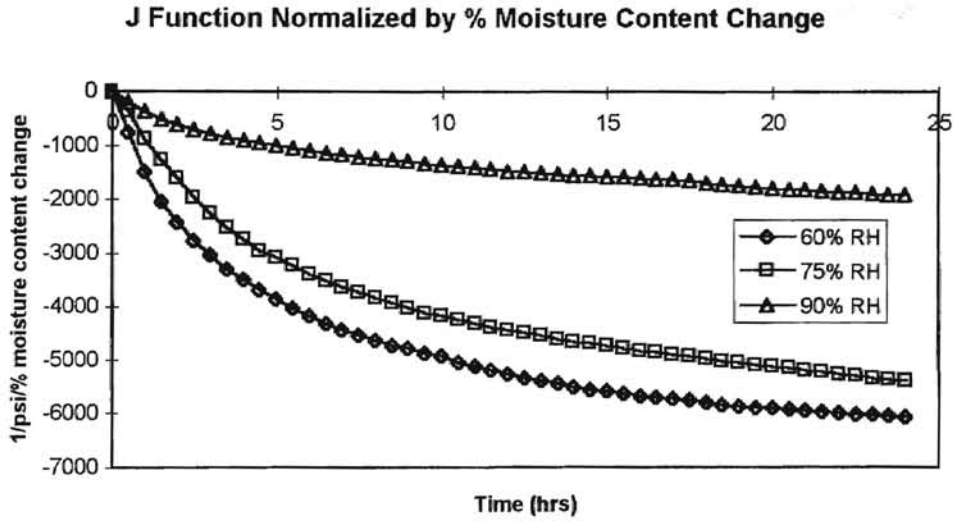

Figure 4.9: Attempt to Normalized J Function

Core Elastic Modulus through Upload Pressure

The core elastic modulus can be calculated from the beginning data of a viscoelastic test. When the core is being uploaded to 50 psi to test viscoelasticity, the strain that the core experiences instantaneously to the 50 psi pressure is the elastic strain. The electronic pressure gauge provided the pressure applied to the core, and the strain

gauge supplied the instantaneous strain data. The pressure versus circumferential strain data were plotted, and the slope of the data is the core modulus.

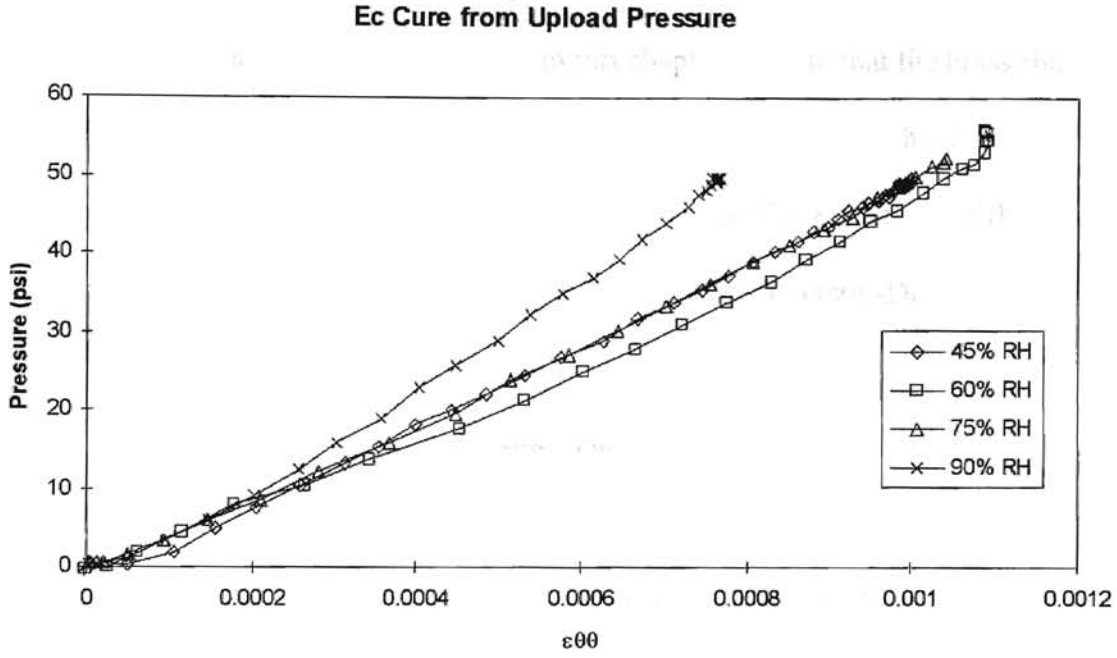

Figure 4.10: Pressure versus Strain Curve of Upload Pressure

	45% RH	60% RH	75% RH	90% RH
E_c (psi)	51000	49000	50000	66000

Table 4.1: E_c from Figure 4.10

These tests showed that the core elastic modulus does not change with humidity change, differing from the results presented at the end of Chapter 3 in which E_c was decreasing with increasing moisture content. According to CCTI [6] the flat crush strength and the axial crush strength of a core decreased as it gains moisture content. Their graphs showed that both flat and axial crush strength decreased about 60% when percent moisture changed from 7.5% to 14%. With that much change to the crush strength of the core, one would expect to see a decrease in the core stiffness as well. The only explanation for the

discrepancy is that the elastic region of the core is not affected by moisture content. Change in moisture content affects the maximum pressure the core can withstand before crushing but does not affects the elastic region of the core.

The E_c data and the viscoelastic data in this chapter indicate that the brass shim transducer can not be used to determine E_c from the procedure used in Chapter 3. Table 3.9 showed that at 90% RH the strain difference between the free expansion of the core ($\varepsilon\theta\theta$-DCDTu) and the expansion of the core under the brass shim ($\varepsilon\theta\theta$-DCDTr) is about 5000 μ-strain. When comparing this to Figure 4.7, most of the 5000 μ-strain can be attributed to viscoelastic property of the core. The pressure calculated between the core and the shim in Table 3.9 was 21 psi. At that pressure and E_c being the 50000 psi (calculated above), the core would only have deflected 420 μ-strain. In order for deflection to reach 5000 μ-strain, as recorded in the 90% RH brass shim transducer test, viscoelastic relaxation must be occurring. Therefore, in order to calculate E_c from the brass shim transducer, the elastic strain and the viscoelastic strain have to be separated. The E_c test performed in this chapter is much more accurate because it measured E_c directly by putting pressure on the core and measuring the strain rather than calculating it from other data.

CHAPTER 5

Hygroscopic Model

Incorporating a New Boundary Condition

As mentioned in the introduction, the purpose of this thesis is to develop a model to predict the interlayer pressure change in a wound roll caused by moisture content change in a wound roll. Hakiel's model was used to achieve this task. The viscoelastic core model was used [4] as an example to develop a time varying model.

Like the viscoelastic model, this model executed Hakiel's model initially to develop a pressure profile. The hygroscopic model then monitored the core dimension change through a step time change. A new pressure profile can be calculated for each updated dimension change using equation (2.2)

To determine the new inner boundary condition affecting the wound roll, consider a core increasing in outer radius due to a change in percent moisture content, and it is restrained by a wound roll. As it expands, the pressure between the first layer of the wound roll and the core will increase. As pressure increases, the core will react with a negative strain on the core due to the elastic modulus. It will also react with a negative strain due to the viscoelastic property of the core. Therefore, to model the dimension change of a core due to percent moisture content changes, the only modification needed to Henning's model was to add the strain due to moisture content change to the viscoelastic boundary condition.

Equation (3.5) describes the strain of the core due to change in percent moisture content,

$$\varepsilon(t) = \frac{\chi}{100} H(t) \tag{3.5}$$

but it describe the total strain of the core at time t. Hakiel's model is interested in incremental change. Therefore, the incremental change of equation (3.5) for a fourth order polynomial is:

$$\varepsilon(t_i - t_{i-1}) = \chi\left[A_4\left(t_i^{\,4} - t_{i-1}^{\,4}\right) + A_3\left(t_i^{\,3} - t_{i-1}^{\,3}\right) + A_2\left(t_i^{\,2} - t_{i-1}^{\,2}\right) + A_1\left(t_i - t_{i-1}\right)\right] \tag{5.1}$$

Adding equation (5.1) into the boundary condition of equation (2.21) yields:

$$r\frac{d\delta \mathrm{P}_{r_1}}{dr} + \delta P_{r_1}\left(1 - \upsilon - \frac{E_t}{E_c}\right) = \left(J_0 + \sum_{n=1}^{2} J_n e^{\frac{-\Delta t}{T_n}}\right)\sigma + \chi\sum_{n=1}^{4} A_n(t_i^{\,n} - t_{i-1}^{\,n}) \tag{5.2}$$

Applying central point difference for first derivative to equation (5.2) yields:

$$\frac{r_1}{h}\delta P_{r_1,t_{i+1}} + \left(1 - \upsilon - \frac{r_1}{h} - \frac{E_t}{E_c}\right)\delta P_{r_1,t_1} = \left(J_0 + \sum_{n=1}^{2} J_n e^{\frac{-\Delta t}{T_n}}\right)\sigma + \chi\sum_{n=1}^{4} A_n(t_i^{\,n} - t_{i-1}^{\,n}) \tag{5.3}$$

The outer boundary condition is assumed to be traction free and zero stress. Therefore, the outer boundary condition is:

$$(\delta P)|_{r=s} = 0 \tag{5.4}$$

The two boundaries are use to solve the governing differential equation

$$\delta P_{i+1}\left(\frac{r_i^{\,2}}{h^2} + \frac{3r_i}{2h}\right) + \delta P_i\left(1 - \frac{2r_i^{\,2}}{h^2} - g^2\right) + \delta P_{i-1}\left(\frac{r_i^{\,2}}{h^2} - \frac{3r}{2h}\right) = 0. \tag{2.8}$$

A tri-diagonal simultaneous equations are set up to solve for a set of interlayer pressure for each time step. Because radial modulus change with pressure, a set of radial modulus

is also calculated for each time step. The solution of the differential equation problem gives a set of pressure profile in the roll for each time step analyzed.

Other Properties to Consider

As discussed in the previous chapter, the viscoelastic property of the core changed dramatically with the change in percent moisture content of the core, almost doubling in change from 45% RH to 60% RH and 60% RH to 75% RH. Therefore, it is important that the correct viscoelastic property be used for the model. Ideally, there would be a creep compliance function for the core while the percent moisture content is changing, but since this information is not available, an estimate is the only other option. Since it is known that the viscoelastic property of the core at 60% RH is twice as much as 45% RH, it could be said that the 60% RH viscoelastic property dominates when a core is going through that change in RH, the same for 60% RH to 75% RH. It is reasonable to assume then that the model will be less accurate at initial time change, because the core will exhibit the 45% viscoelastic property. The problem with using viscoelastic property at certain RH is that the creep compliance function is not in the same time frame as the humidity compliance function. The humidity compliance function represents the strain of the core as moisture content is changing. The creep compliance function represents the viscoelastic strain of the core once it has reached equilibrium with the environment.

Henning's inner boundary equation (2.21) was created for a linear viscoelastic core. In order for a material to be linear viscoelastic, the strain the material exhibits has to normalize when divided by the applied pressure, hence producing a creep compliance function. Henning proved in his research that the paperboard cores he tested were linearly

viscoelastic. This paper assumes that the paperboard cores tested in this research were also linear viscoelastic. That is the reason why only one pressure was tested to produce the creep compliance functions in Chapter 3.

Another problem to consider is that the creep compliance function could not be normalized with the moisture change. Therefore, the strain due to viscoelasticity can not be calculated for every percent moisture content change. In order to use the model, the viscoelastic property of that humidity change has to be known. There are only data for 45% to 60%, 60% to 75%, and 75% to 90% RH change (The 75% to 90% RH is not consistent with the other data. Hence, the reliability of this data is not determinable). Only those changes in RH can be modeled.

The H(t) function, developed in Chapter 3, was developed from tests in which both the outside and the inside of the core were exposed to the environment. A wound roll impeded the rate at which moisture can penetrate the outer surface of the core, changing the rate at which the core absorbed moisture. Therefore, the H(t) function has some unpredictable error built into it when applied to a wound roll. From data gathered in Chapter 3, it is safe to assume the core will reach the same dimension change once it reaches the same moisture content.

Computer Model

A viscoelastic program that Henning wrote was easily modified to solve the finite difference problem above. Only a couple of lines were changed and added to his program. The FORTRAN code is listed in appendix B. The flow diagram of program is shown in Figure 5.1.

Input require by program:

- winding tension
- outside radius of core
- outside radius of core roll
- number of laps through roll
- total time to model
- number of increment through the total time
- radial modulus of core
- Poisson's ratio of core
- radial modulus of web
- tangential modulus of web
- Poisson's ratio of roll
- creep compliance function for humidity change
- humidity compliance function
- percent moisture content change

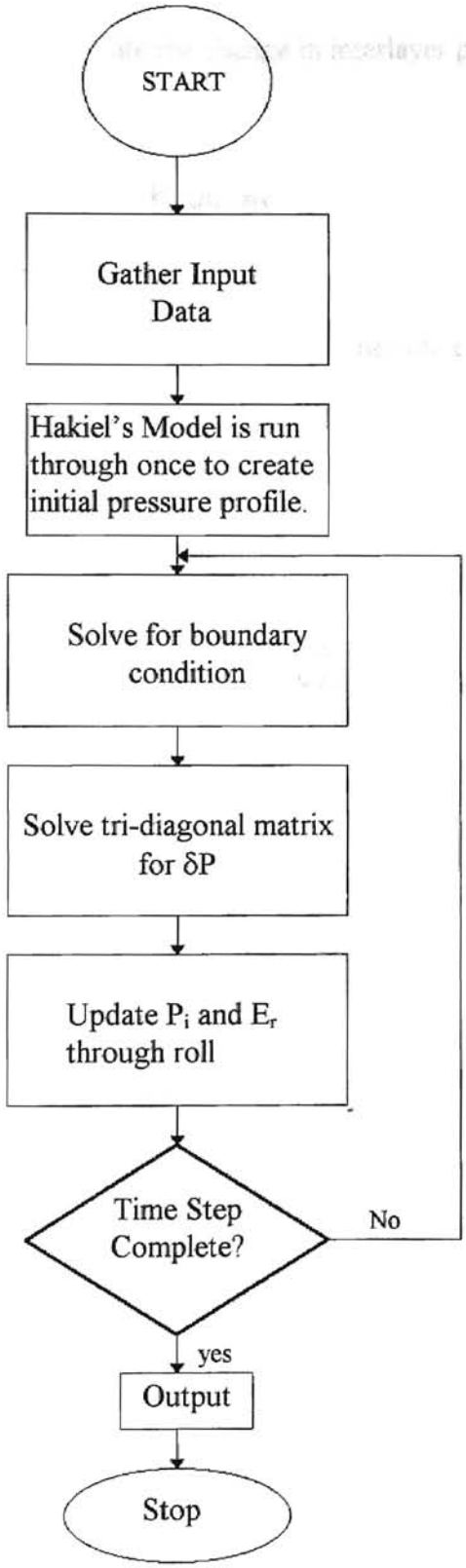

Figure 5.1: Flow Diagram

The program is designed to calculate the change in interlayer pressure of a wound roll due to a step change in percent moisture content. Input to the program can be entered through a keyboard or an input file. If data are input through the keyboard, a file of the input is written. The program creates two output files. One file contains the interlayer pressure of the wound roll for each time step. The other file contains data on how the core and first web interlayer pressure changes through time.

The following conditions were input into the model in order to analyze it response.

Winding Tension	900 psi
Roll Inside Radius	1.7 inch
Roll Outside Radius	4.2 inch
% Moisture Content Change	.0084 (or 45% to 60% RH change)
Roll Iteration	500
Time Iteration	100
Time Change	2000 minutes
ICI 377 48 Gauge Film	
E_r	$.0005P^3 - .1903P^2 + 37.051P$ (psi)
E_t	600,000 psi
μ_s	.21
Core Properties	
E_c	50,000 psi
Creep Compliance Function	
45% RH	$J(t) = -24.38 + 5.16e^{-t/76.75} + 19.22^{-t/856.32}$
60% RH	$J(t) = -52.67 + 16.74e^{-t/86.28} + 35.92^{-t/505.65}$
Humidity Compliance Function	
	$H(t) = -1(10^{-8})t^4 + 8(10^{-5})t^3 - .2122t^2 + 265.49t$

The creep compliance function for both RH condition are modeled. The two results will be compared to see how they differ.

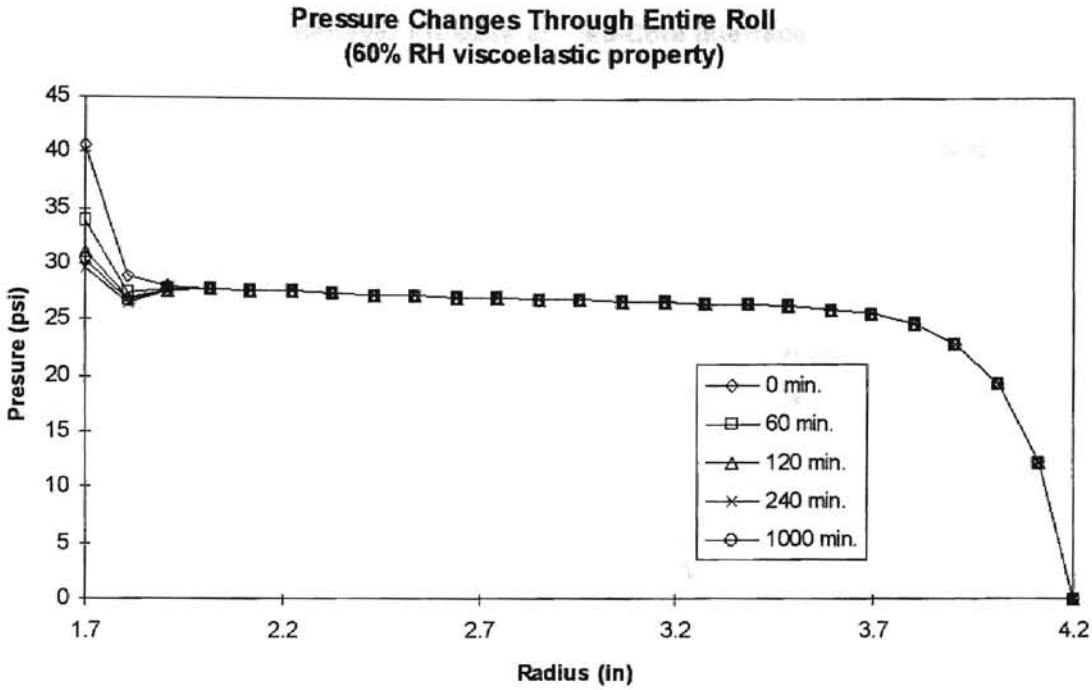

Figure 5.2: Interlayer Pressure in Roll of 900 psi Winding Tension and 60% RH Viscoelastic Property

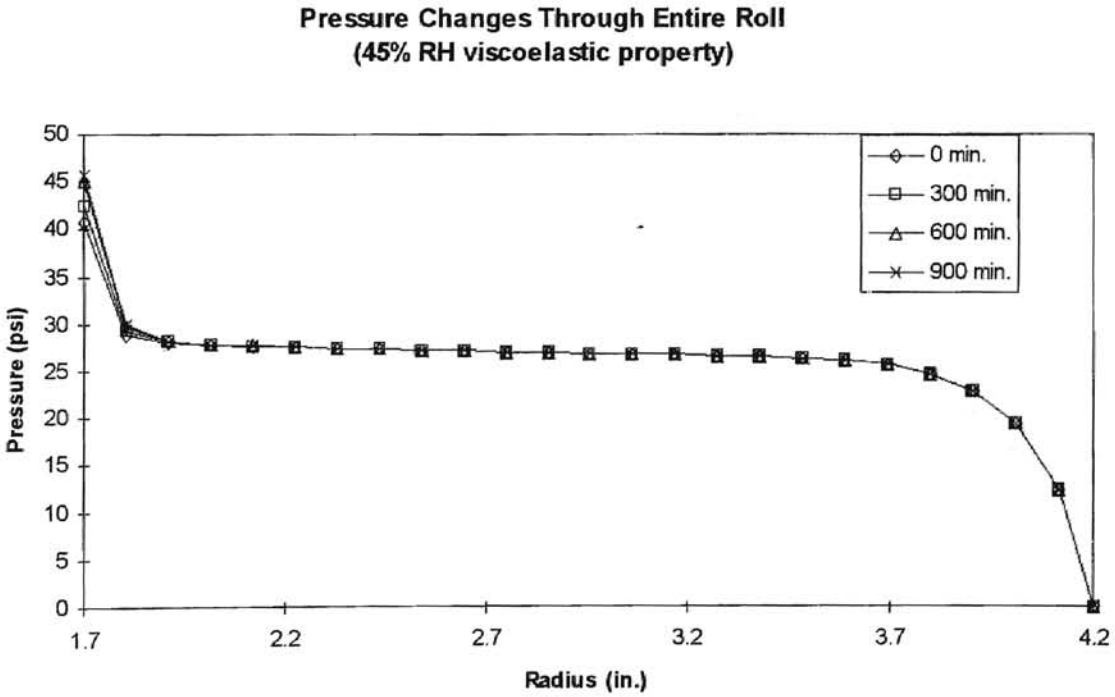

Figure 5.3: Interlayer Pressure in Roll of 900 psi Winding Tension and 45% RH Viscoelastic Property

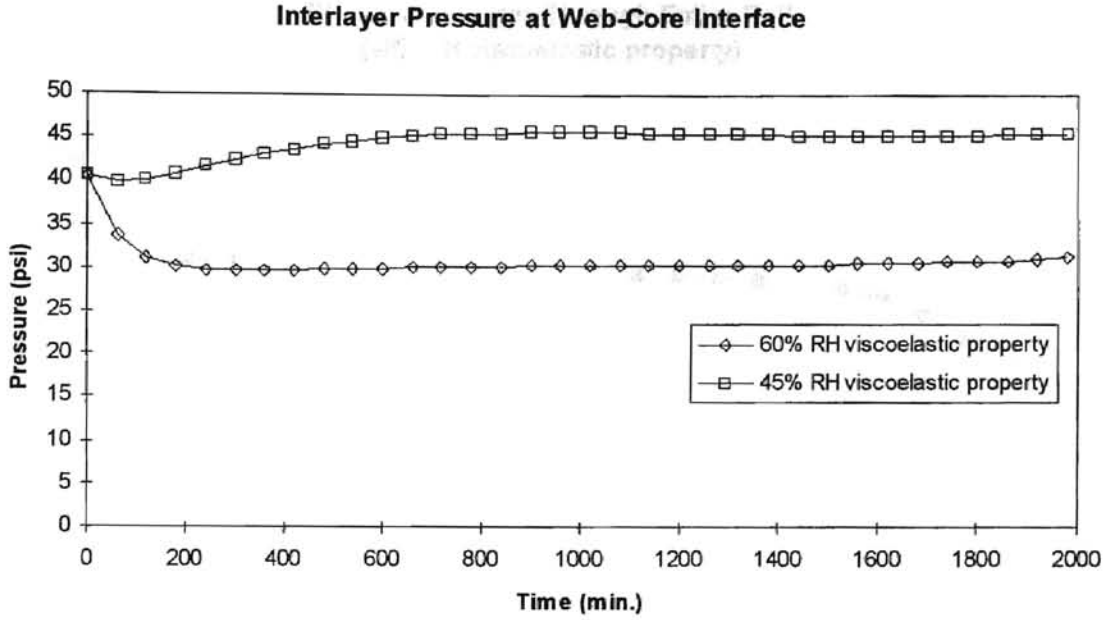

Figure 5.4: Interlayer Pressure at Web-Core Interface (900 psi Winding Tension)

The web tension was changed to 1200 psi, and the following data was collected from the model.

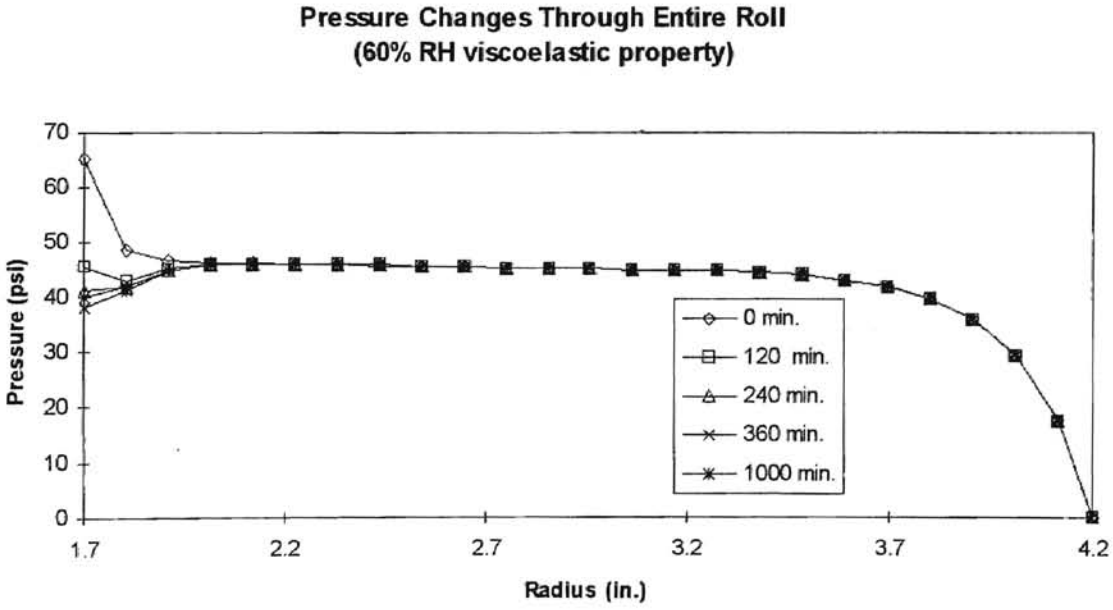

Figure 5.5: Interlayer Pressure in Roll of 1200 psi Winding Tension and 60% RH Viscoelastic Property

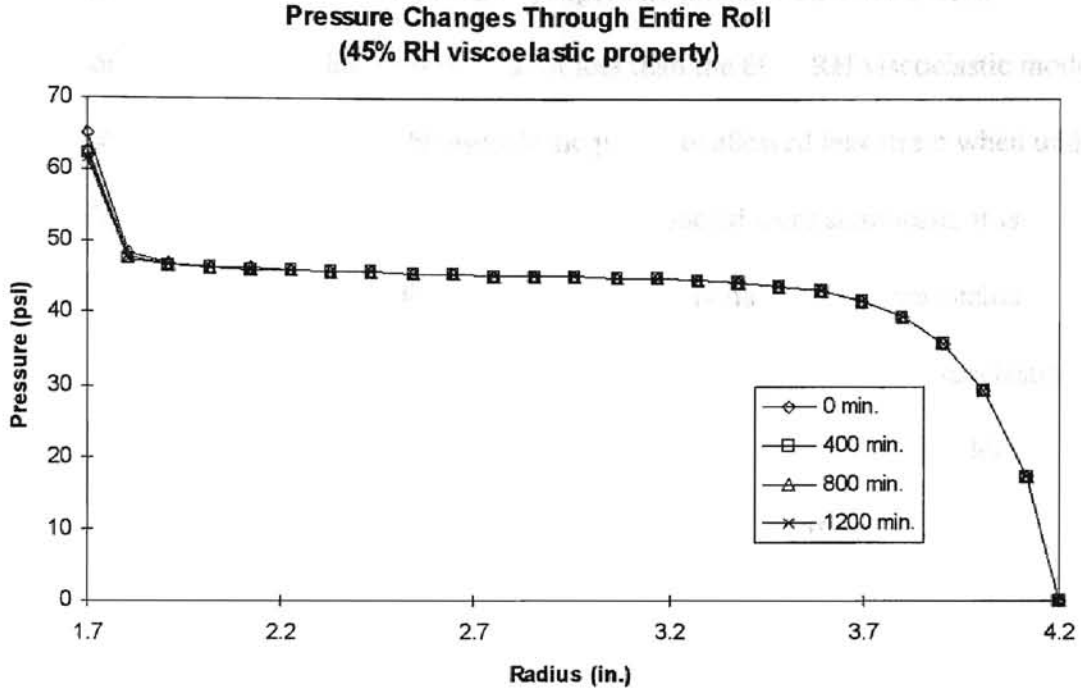

Figure 5.6: Interlayer Pressure in Roll of 1200 psi Winding Tension and 45% RH Viscoelastic Property

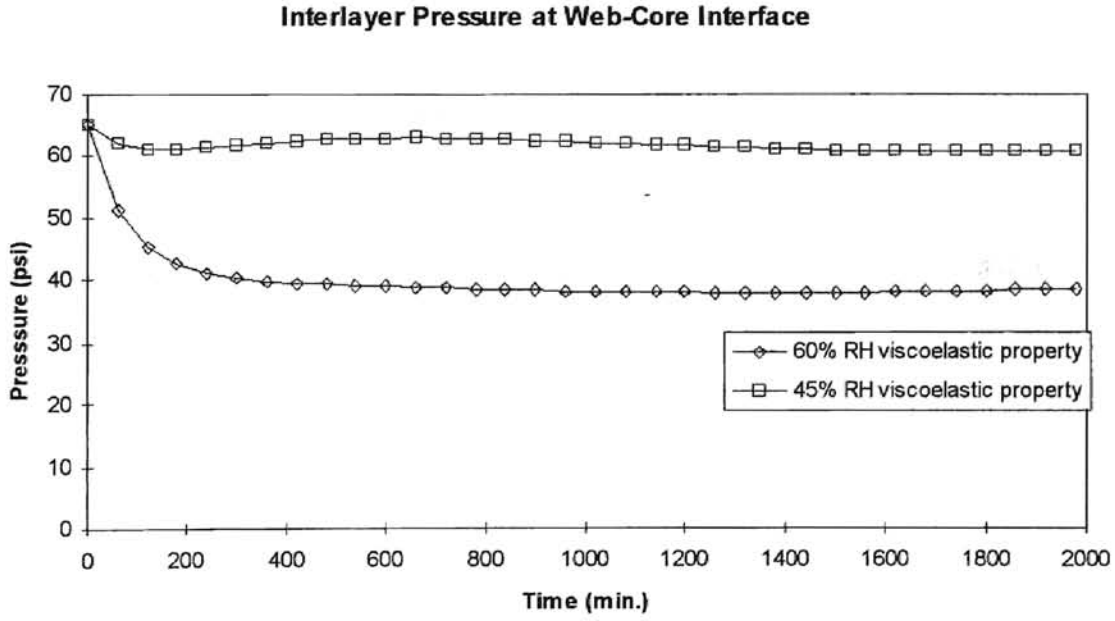

Figure 5.7: Interlayer Pressure at Web-Core Interface (1200 psi Winding Tension)

When comparing the two viscoelastic properties, the 45% RH viscoelastic property model changed interlayer pressure a lot less than the 60% RH viscoelastic model. This is expected because the 45% RH viscoelastic property allowed less strain when under pressure. The differences in the two properties when modeled were significant, it is reasonable to assume that the 45% RH viscoelastic property model represents actual interlayer pressure at the initial time change of the model, and the 60% RH viscoelastic model represents the actual pressure at a later time change. The time in the model when the 45% RH viscoelastic property switched to the 60% RH viscoelastic property is unknown.

All the runs so far have been for situation where the core was gaining moisture. This is because the humidity compliance function was developed from data where the core was gaining moisture. As shown in Table 3.7, however, the dimensional change of the core per unit change in moisture content remained relatively constant through a wide range of humidity conditions. Therefore, it could be hypothesized that for conditions when the core is losing moisture the same humidity compliance function applies. The strain due to decrease in moisture content of the core could be determined by multiplying the humidity compliance function by a negative moisture content change.

Using the above theory, the following conditions were input into the program to analyze the model response for a core drying from 90% RH to 0% RH.

Winding Tension	1200 psi
% Moisture Content Change	-14.22 (90% to 0 % RH)
Time Change	100 minutes
Creep Compliance Function	
90% RH	$J(t) = -108.6 + 28.79e^{-t/115.93} + 79.81e^{-t/1516.6}$
(assuming that 90% RH properties dominate)	

(All other properties were the same as previous runs.)

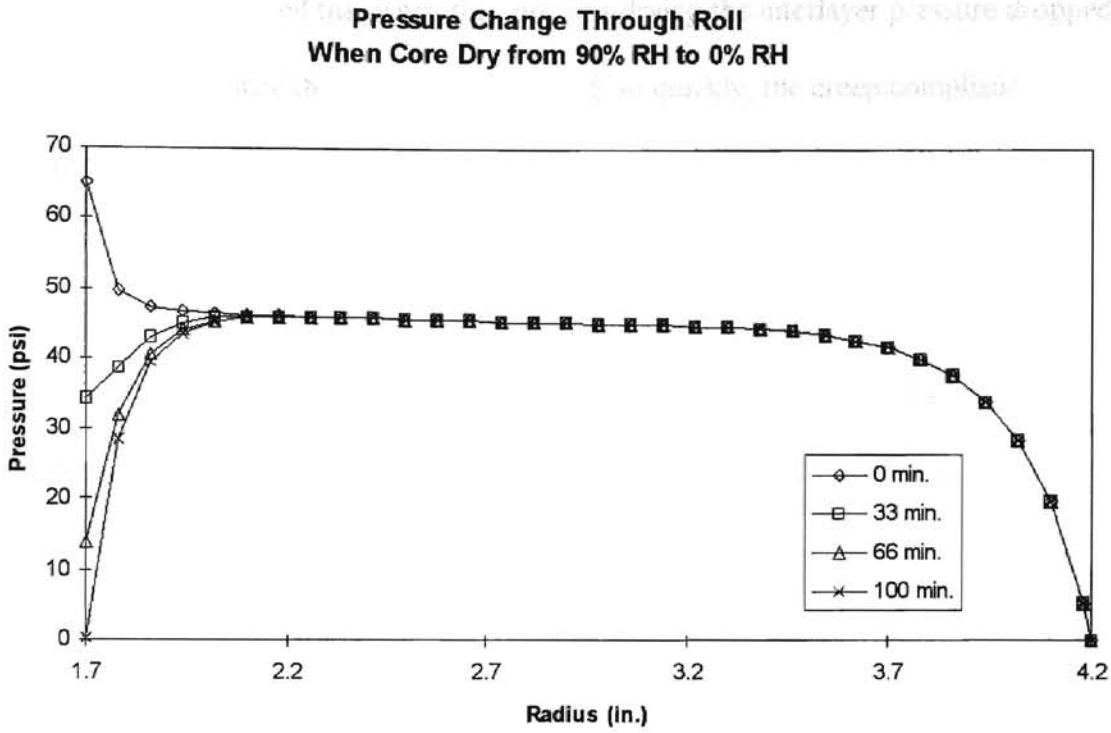

Figure 5.8: Interlayer Pressure in Roll When Core is Drying

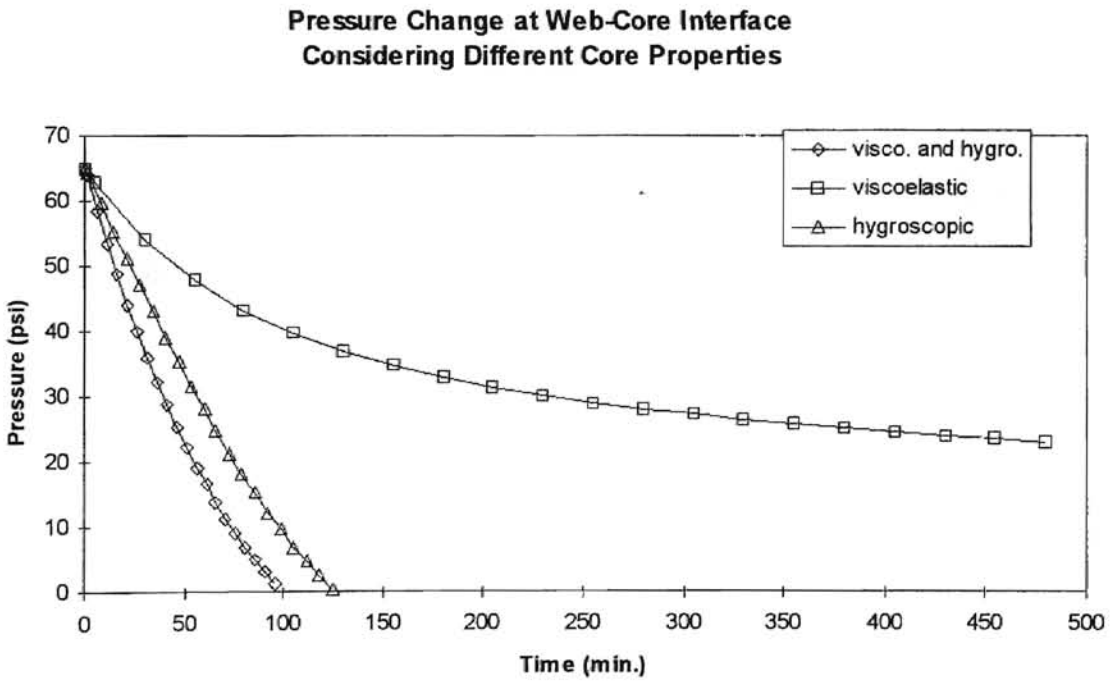

Figure 5.9: Pressure Change at Web-Core Interface

The model showed that when the core was drying the interlayer pressure dropped off rather quickly. Since the pressure dropped off so quickly, the creep compliance function probably did not have enough time to significantly change from it 90% RH condition. Therefore, the assumption made above to use the 90% RH creep compliance function, closely predicted the actual condition of the core.

The model indicated that change in the boundary condition caused a very localized pressure change in the wound roll. Only the web 0.3 inch from the core was affected by the dimensional change. Web material outside the 0.3 inch had no reaction to the boundary change. The first layer of web experienced the greatest change to its pressure. The localized pressure changes correlate Henning's data.

Experiments to verify the condition mentioned above were done before the model was available. A wound roll was created to the specified conditions and allowed to go through the humidity change. A punch test was used to determine the interlayer pressure before and after the humidity change. The punch test was developed by Hakiel to verify his model. The punch test determined the interlayer pressure by forcing two layers of web to slip past one another. Knowing the static coefficient of friction, the interlayer pressure can be calculated by knowing the force needed to make the layers slip past one another.

$$P = \frac{F}{2\pi r_{slip} w \mu_s} \qquad (5.5)$$

Equation (5.5) calculates the interlayer pressure from the punch force.

	Experimental Pressure (psi)	Theoretical Pressure (psi)	Pressure Hygroscopic Effect only (psi)	Pressure Viscoelastic Effect only (psi)
Winding Tension 900 (psi)	1.95 inch In-Roll Radius			
Time=0 (min.)	30.63	27.96	27.96	27.96
Time=2000 (min.)	27.56	27.72	28.7	27.37
Winding Tension 1200 (psi)	1.95 inch In-Roll Radius			
Time=0 (min.)	48.5	46.65	46.65	46.65
Time=1238 (min.)	46.73	45.37	48.19	44.76

Table 5.1: Verification of Model (45% RH to 60% RH)

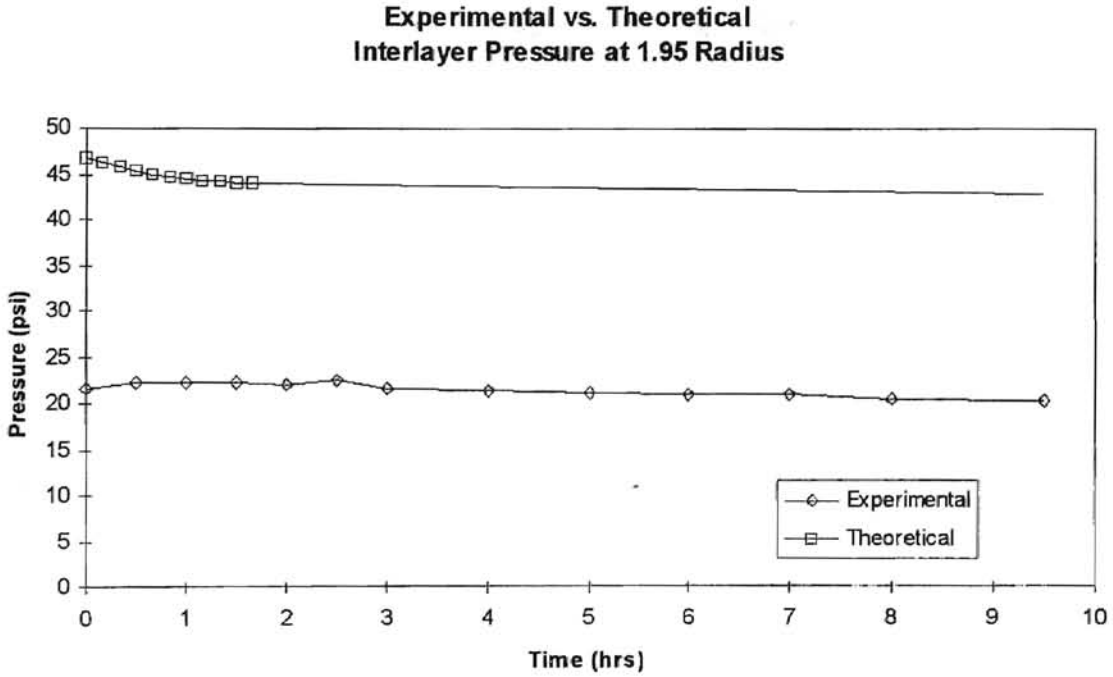

Figure 5.10: Verification of Model (90% RH to 0% RH)

For the case when the core was gaining moisture, the theoretical and experimental data agree to within 10%. For the case when the core was losing moisture, the theoretical pressure change was twice that of the experiment. An explanation for this was that the model can only predict pressure change after winding. If pressure dropped at the core

web interface during winding, this might account for the pressure difference between the model and the experimental data. Unfortunately, the punch test only allowed tests at one radius for each die. Only one punch die was available to do the test. Therefore, only 1.95 inch in-roll radius pressure data were acquired.

The run in which the viscoelastic or the hygroscopic properties were modeled showed that when the core was gaining moisture the hygroscopic and the viscoelastic properties fight each other in affecting the wound roll pressure. The hygroscopic property increased the pressure within a wound roll, while the viscoelastic property decreased the pressure. In this case, the viscoelastic property is the dominant property. When both property were account for, the interlayer pressure of the wound roll decreased similarly to the viscoelastic property. In the case in which the core lost moisture, the hygroscopic property and the viscoelastic property worked together decreasing the pressure in a wound roll. As the core pressure decreased the viscoelastic property became less of a factor affecting the roll pressure, therefore, the hygroscopic property is the dominant factor in this case.

CHAPTER 6

Conclusions

The goal of this study was to create a model that could predict the interlayer change in a wound roll due to dimension changes of the core caused by moisture content changes. To accomplish this goal required that the core behavior as a function of moisture content be understood.

It was determined that change in moisture content of the core was related to change in the RH of the air. CCTI gave data on how these properties were related (Table 2.2). Tests were done to see if these data were reproducible. As Table 3.6 showed, the data gathered from this research were very close to CCTI data, with maximum discrepancy of 2% at 90% RH.

An experiment was setup to determine how the dimensions of the cores related to different core moisture content. When all the data were collected, it was found that the dimension change of the cores could be normalized by the change in percent moisture content. This information allowed the prediction of the dimension change of the core due to any positive change in percent moisture content of the core. When the core dimension change was compared with CCTI, the discrepancy between the two data sets was significant. The data from this research were twice as high as predicted by CCTI. Of course, CCTI only gives a guideline to follow when trying to predict dimension change in core due to moisture content change. The cores that CCTI tested must have had different

properties than the cores tested for this research. Even though the two data sets do not agree, both steps do agree that the diametral growth of a paperboard core per percentage moisture content change is nearly constant through a wide range of RH levels.

When the model was being developed, it was theorized that if the core was to increase in size, it would cause the pressure to increase around it. This increase in pressure would also cause the core to viscoelastically deform at a greater rate. Therefore, data on the viscoelastic properties of the core at different humidity were also needed. Experiments on this property showed that it changed dramatically at different humidity conditions. It was found that the relaxation functions for the cores at various moisture contents could not be normalized. This complicates the analysis, because it did not allow the prediction of the viscoelastic properties of the core at different moisture contents by simple linear viscoelastic theory.

When all the core boundary conditions were considered, a model was created to predict the pressure change. The model showed the core viscoelastic property to be the dominating factor affecting the pressure of the wound roll when the core gained moisture. When a core increased in size due to an increase in moisture content, it was suspected that this would cause an increased pressure around the core, but the model showed that the pressure was decreasing with time instead of increasing. This can be attributed to the viscoelastic property dominating over the growth property of the core. When the core was losing moisture, however, both the viscoelastic and the hygroscopic properties work together to decrease the pressure of the wound roll. As pressure decreased the viscoelastic property became less important to the pressure within the wound roll, and the hygroscopic properties dominate the wound roll pressure. The model also showed that

the pressure change is localize to the web near the core. The changes at the core does not affect the wound roll more than 0.3 inch from the core.

CHAPTER 7

Future Work

The model in this paper was developed with the assumption that the higher humidity viscoelastic property dominates when a core is changing moisture content. The model would be more accurate if the viscoelastic property of the core could be measured while the core is changing moisture content. This would result in the growth data and the viscoelastic data being in the same time frame.

Future work to predict the viscoelastic property of the core at different humidity is also needed. Presently, there is no procedure for predicting the different viscoelastic properties at different core moisture contents. A viscoelastic test has to be done for each humidity condition that the core is expected to change to, but this is not very efficient. A procedure is needed to predict the viscoelastic properties at all humidity conditions from a few tests.

More verification work is also needed for the model. Though some verification was done for the model. Only a few points were acquired to verify the model. More verification nearer to the core is needed to better prove the model.

H(t) should be measured for conditions similar to that found in a wound roll. In this research, H(t) was calculated from data where both outer and inner surface of the core were exposed to the environment. Then, the same H(t) was used to model a wound roll in which the outer surface was wrapped by web that impeded moisture from penetrating the

outer surface. Future work might consider coating the core with a material impermeable to moisture before measuring H(t). This would give a more accurate H(t) when modeling the wound roll with web material impermeable to moisture, such as plastic film. A semi-permeable coating for the core could be used to measure H(t) when modeling web material like paper that slow the time it take for moisture to penetrate the core.

BIBLIOGRAPHY

[1] Beckwith, Thomas G., Marangoni, Roy D., & Lienhard, John H.V., Mechanical Measurement, 5th ed., Addison-Wesley, New York, 1993.

[2] "The Effect of Moisture Content on Dimensional Stability and Strength Properties of a Typical Paperboard Tube or Core", Composite Can and Tube Institute, June 1989.

[3] Etter, D. M., Structured FORTRAN 77 for Engineers and Scientists, 4th ed., Benjamin/Cummings, California, 1993.

[4] Findley, William N., Lai, James S., & Onaran, Kasif, Creep and Relaxation of nonlinear Viscoelastic Materials, North Holland Publishing Company, New York, 1976.

[5] Gerald, Curtis F., & Wheatley, Patrick O., Applied Numerical Analysis, 5th ed. Addison-Wesley, Massachusetts, 1994.

[6] Gerhardt, T.D., Qiu, Y.P., "Paper Tube Deformation During Winding Processes", Mechanics of Cellulosic Materials, MD-Vol 36, 1992.

[7] Hakiel, Z., "Nonlinear Model for Wound Roll Stresses", Tappi Journal, May 1987

[8] Henning Jeffrey S., "Effect of Relaxation of a Core on a Wound Roll", Master Diss., Oklahoma State University, May 1995.

[9] Measurement Group, "Strain Gage Conditioner and Amplifier System Instruction Manual", North Carolina, 1992.

[10] MetraByte, "Dash-16/16F Manual", Massachusetts, 1986.

[11] National Instruments, "Instrumentation Reference and Catalogue", 1997 ed., Texas, 1996

[12] Quall, William R., & Good, J. Keith, "Thermal Analysis of a Wound Roll", OSU Wed Handling Research Center.

[13] Quall, William R., "Hygrothermomechaincal Characterization of Viscoelastic Center Wound Roll", Ph.D. Diss., Oklahoma State University.

[14] Roisum, David R., "Moisture Effects on Webs and Rolls", Finishing and Converting Conference, 1992.

[15] Roisum David R, "The Measurement of Web Stresses During Roll Winding", Ph.D. Thesis, Web Handling Research Center at Oklahoma State University, May 1990.

[16] Shigley, Joseph E., & Mischke, Charles R., Mechanical Engineering Design, 5th ed., McGraw-Hill, New York, 1989.

[17] Rosenberg & Karnopp, Introduction to Physical System Dynamics, McGraw-Hill, New York, 1983.

APPENDIX A

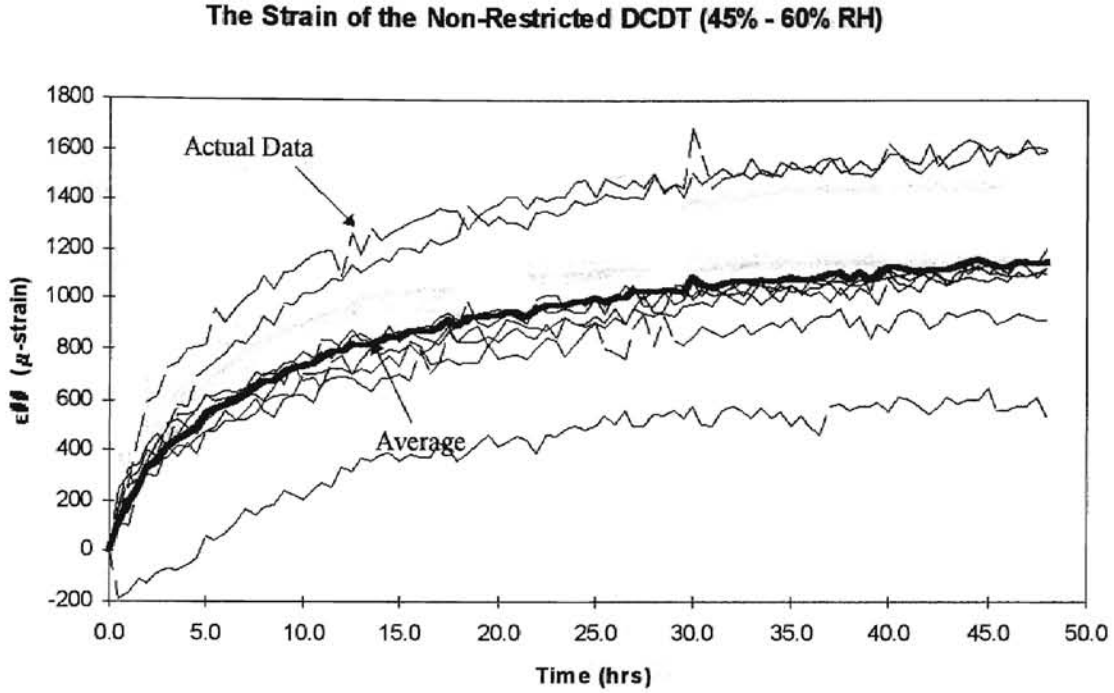

Figure A.1: Actual and Average Data of Expansion of Core (45% - 60% RH)

Note: The light lines are actual experimental data of core growth. The dark line is average of those data.

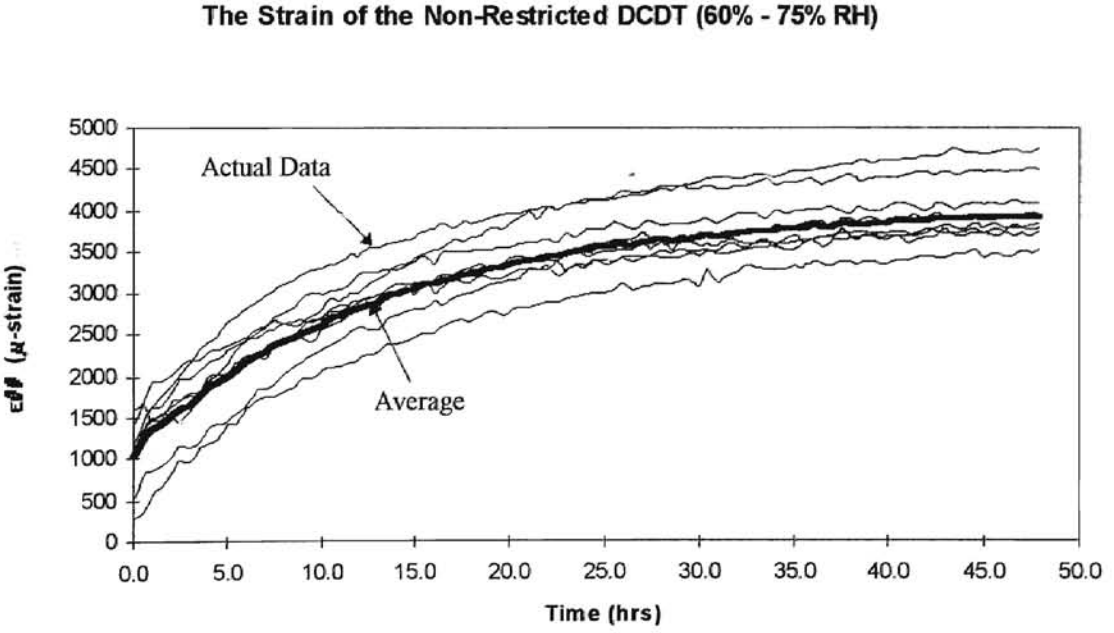

Figure A.2: Actual and Average Data of Expansion of Core (60% - 75% RH)

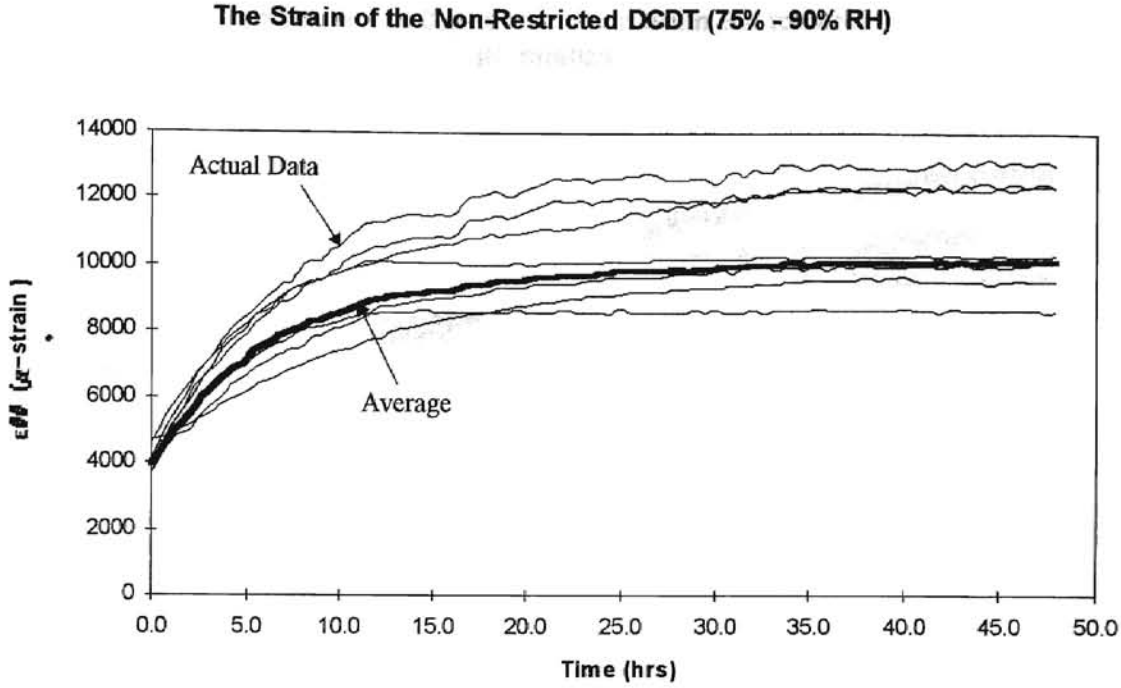

Figure A.3: Actual and Average Data of Expansion of Core (75% - 90% RH)

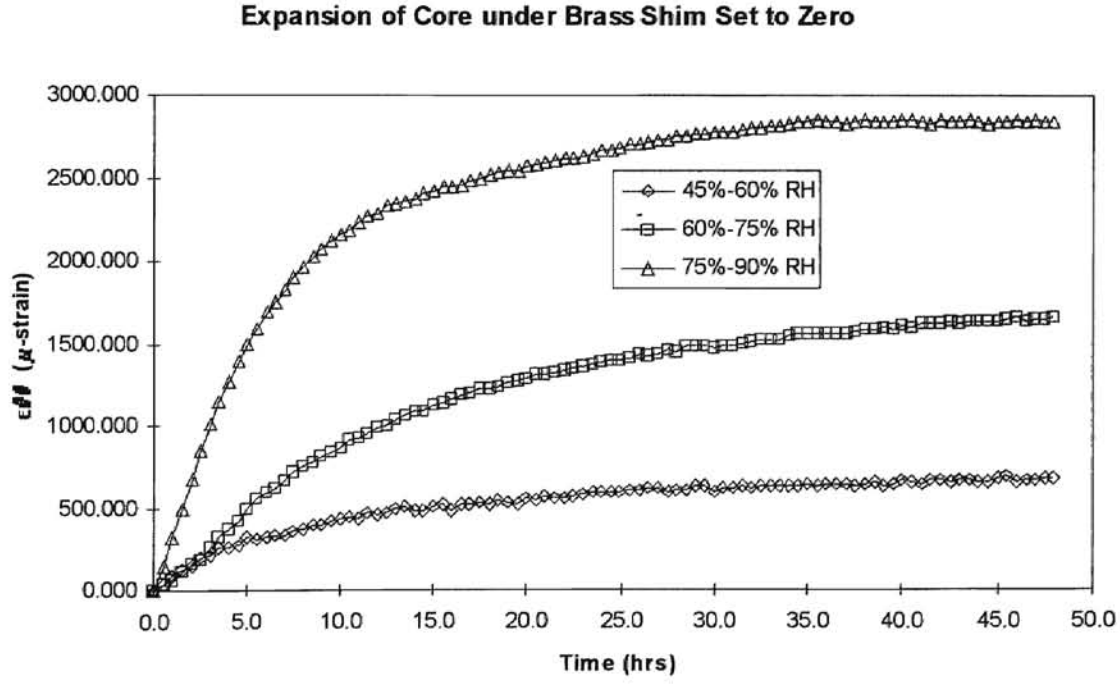

Figure A.4: Expansion of Core under Brass Shim

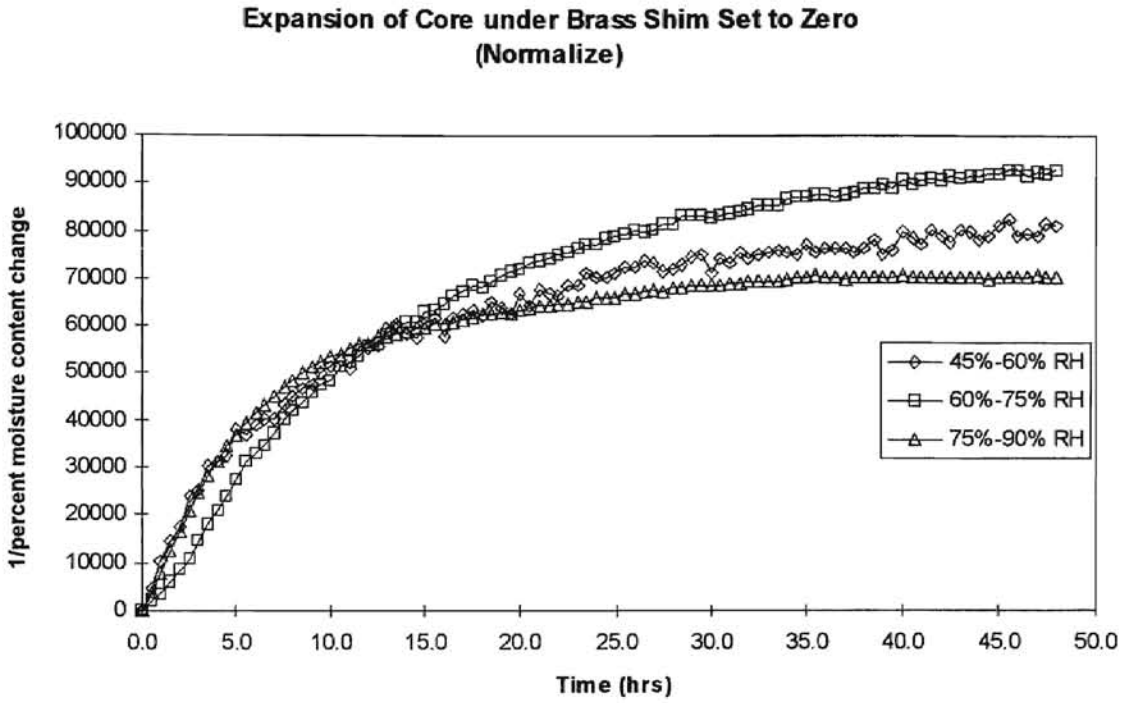

Figure A.5: Normalized Expansion of Core under Brass Shim

APPENDIX B

```
**********************************************************************
**********************************************************************
**********************************************************************
*****                                                            *****
*****          HYGROSCOPIC EFFECT ON CORE                        *****
*****               1st ed.                                      *****
*****           Modified By:  Hung Nguyen                        *****
****      Main Program By: Jeff Henning                          *****
*****          Project Coordinator: Dr. J. Keith Good           *****
*****                                                            *****
***** Web Handling Research Labotratory (WHRC)                  *****
***** Oklahoma State University                                 *****
***** Deptartment of Mechanical and Aerospace Engineering        ****
***** Stillwater, Oklahoma                                      *****
*****                                                            *****
*****  Calculates Stresses Induced Due to the                   *****
***** Expansion of the Core Due to                              *****
***** Increase Percent Moisture Content                         *****
*****                                                            *****
**********************************************************************
**********************************************************************
**********************************************************************
**
***** Main Program Corerelax
***** -opens and closes input/output files
***** -make calls to subroutine
**
**********************************************************************
      PROGRAM CORERELAX
      OPEN(1,FILE='CORECRH.IN')
      OPEN(2,FILE='CORECRH.OUT')
C     OPEN(3,FILE='CORSTH.OUT')
      OPEN(4,FILE='COREPRH.OUT')
      OPEN(5,FILE='LPRES.OUT')
      WRITE(*,*)'*******************************************************'
      WRITE(*,*)'ENTER "1" FOR FILE INPUT OR "0" FOR KEYBOARD INPUT'
      READ(*,*)IANS
      WRITE(*,*)'*******************************************************'
      IF(IANS.EQ.0) THEN
      CALL UINPUTS
      ELSE
      CALL INPUTS
      ENDIF
      WRITE(4,120)
      WRITE(*,*)'*****Calculating*****'
```

```
      CALL WINDER
      CALL RELAX
      WRITE(*,*)'*****Finished*****'
      WRITE(*,*)'*************************************************'
C     CALL OUTS
120   FORMAT('   TIME        PRESSURE    DELTA        B(1)')
      CLOSE(2)
C     CLOSE(3)
      CLOSE(4)
      CLOSE(5)
      STOP
      END
*********************************************************************
*********************************************************************
*********************************************************************
**
***** Subroutine RELAX
*********************************************************************
      SUBROUTINE RELAX
      IMPLICIT REAL*8 (A-H,J,O-Z)
      COMMON/PARAM/RINC,RIN,ROUT,NLAPS,NINC,NCORE,WT
      COMMON/CLOCK/DCLOCK,U(1000),DTP(1000),NCLOCK,J0,J1,T1,J2,T2
      COMMON/MATLPROP/EC,E,vc,ET,AA(0:3),ER(1000),vrt,vtr
      COMMON/TIME/R(1000),TIME,TWIND,LAP,DTOLD,DTIME
      COMMON/MATCOEFF/A(1000),B(1000),C(1000),D(1000),N
      COMMON/PRES/P(1000),DP(1000),S,OLDP,VP(1000)
      COMMON/HUMID/X,HA0,HA1,HA2,HA3,HA4


C     WRITE(*,*)'RELAX IN OK'
C
CCCCC
C
C     WRITE(3,110)
C     WRITE(4,120)
C     WRITE(*,*)J0
C     J0=J0+1D0/EC
C     WRITE(*,*)J0
      R(1)=RIN
      LAP=1
      H=(ROUT-RIN)/NLAPS
      DO I=2,NLAPS+1
      R(I)=R(1)+(I-1)*H
      END DO
C
```

```
CCCCC
      DO L=1,NLAPS
      VP(L)=P(L)
      END DO

      OLDP=0
C
C     WRITE(*,*)EC,ET
      DCLOCK=DCLOCK/NCLOCK
      DO 999 K=1,NCLOCK
      TIME=K*DCLOCK
      WRITE(2,100)TIME
C     WRITE(*,*)'1ST IN OK'
C
C
ccccccccccccccccccccccccccccccccccc
CCCC  THIS IS STRESS FORMULATION WITH EC
C
CCC   CORE BOUNDARY CONDITION
C
C     A(1)=0D0
      D(1)=(1D0-vrt-Et/(Ec*RIN)-RIN/H)
C     D(1)=(1d0-Et/Er(1)*vtr-Et/(Ec*rin))
      C(1)=rin/h
      S=-(P(1))
      TTEMP=TIME-DCLOCK
      TP1=S*(J0+J1*EXP(-TIME/T1)+J2*EXP(-TIME/T2))
      TP2=S*(J0+J1*EXP(-TTEMP/T1)+J2*EXP(-TTEMP/T2))
      TP3=X*(HA4*TIME**4+HA3*TIME**3+HA2*TIME**2+HA1*TIME+HA0)

TP4=X*(HA4*TTEMP**4+HA3*TTEMP**3+HA2*TTEMP**2+HA1*TTEMP+HA0)
      B(1)=((TP1-TP2)+(TP3-TP4))*Et*.000001
      OLDP=S
C     B(1)=Et*S*(J0+J1*EXP(-TIME/T1)+J2*EXP(-TIME/T2))
C
CCC   ROLL ANALISIS
C
      DO 60 I=2, NLAPS
C     vtr=vrt*Er(I)/Et
C     A(I-1)=(R(I)**2/H**2-R(I)/(2D0*H)*(3d0-Et/Er(I)*vtr+vrt))
C     D(I)=(1D0-2D0*R(I)**2/H**2+vrt-Et/Er(I)*(1+vtr))
C     C(I)=R(I)**2/H**2+R(I)/(2D0*H)*(3d0-Et/Er(I)*vtr+vrt)

      A(I-1)=(R(I)**2/H**2-3D0*R(I)/(2D0*H))
      D(I)=(1D0-2D0*R(I)**2/H**2-Et/Er(I))
```

```
      C(I)=R(I)**2/H**2+3D0*R(I)/(2D0*H)
C
      B(I)=0D0
C
60    CONTINUE
C
CCC   OUTER BOUNDARY CONDITION
C
      D(NLAPS+1)=1D0
C     C(NLAPS+1)=1D0
      B(NLAPS+1)=0D0
      A(NLAPS)=0D0
C
C     WRITE(5,200)TIME
C     DO I=1,NLAPS+1
C        WRITE(5,210)R(I),A(I),D(I),C(I),B(I)
C     ENDDO
C
CCC   SOLVE MATRIX FOR PRESSURES AND PRINT
C
      CALL SOLVETRI(DTP,NLAPS+1)
      LAP=NLAPS+1
      CALL VTOTPRESS(DTP)
      CALL OUTS
      IF (P(1).GT.-1.0.AND.P(1).LE.0.0) THEN
      CALL POUT
      ENDIF
C     CALL STRAIN
999   CONTINUE
C

C 210  FORMAT(F8.2,' ',F15.5,' ',F15.5,' ',F15.5,' ',F15.5)
C 200  FORMAT('TIME = ',F10.1)
100   FORMAT('TIME =',F7.0,' (MIN)')
C   110FORMAT('  TIME     STRAIN        VISCO         ELASTIC')
C   120FORMAT('  TIME     PRESSURE   DELTA    B(1)')
C     WRITE(*,*)'THSTRESS OUT OK'
      RETURN
      END
**********************************************************************
**********************************************************************
*****Subroutine Strain
*****Solves the strain at the first layer of roll
*****  which is equal to the strain of the core
**********************************************************************
```

```
      SUBROUTINE STRAIN
      IMPLICIT REAL*8 (A-H,J,O-Z)
      COMMON/PARAM/RINC,RIN,ROUT,NLAPS,NINC,NCORE,WT
      COMMON/CLOCK/DCLOCK,U(1000),DTP(1000),NCLOCK,J0,J1,T1,J2,T2
      COMMON/MATLPROP/EC,E,vc,ET,AA(0:3),ER(1000),vrt,vtr
      COMMON/TIME/R(1000),TIME,TWIND,LAP,DTOLD,DTIME
      COMMON/MATCOEFF/A(1000),B(1000),C(1000),D(1000),N
      COMMON/PRES/P(1000),DP(1000),S,OLDP,VP(1000)
      COMMON/STRN/VSTRN,ESTRN,TSTRN

C     WRITE(*,*)'STRAIN IN OK'
C     VSTRN=VSTRN+((J0+J1*EXP(-TIME/T1)+J2*EXP(-TIME/T2)*OLDP)
C     ' *1000000)

      VSTRN=VSTRN+B(1)


C     B(1)=Et*S*(J0+J1*EXP(-TIME/T1)+J2*EXP(-TIME/T2))
      ESTRN=(P(1)/EC)*1000000
      TSTRN=(VSTRN+ESTRN)
C     WRITE(3,40)
C     WRITE(3,50)TIME,TSTRN,VSTRN,ESTRN,B(1)
C  40 FORMAT('    TIME    STRAIN ')
50    FORMAT(F10.2,' ',F15.4,' ',F15.4,' ',F10.4,' ',F12.4)
      RETURN
      END
*****************************************************************
*****************************************************************
***** Subroutine SOLVETRI
***** -SOLVES THE TRIDIAGONAL SYSTEM OF DIMENSION IDIM
*****   FOR THE SOLUTION VECTOR X(IDIM)
*****************************************************************
      SUBROUTINE SOLVETRI(X,IDIM)
      IMPLICIT REAL*8 (A-H,J,O-Z)
      INTEGER IDIM
      DIMENSION X(1000)
      COMMON/MATCOEFF/A(1000),B(1000),C(1000),D(1000),N
C     WRITE(*,*)'SOLVE IN OK '
      N=IDIM
      DO 900 I=2,N
      D(I)=D(I)-(A(I-1)/D(I-1))*C(I-1)
      B(I)=B(I)-(A(I-1)/D(I-1))*B(I-1)
900   CONTINUE
      X(N)=B(N)/D(N)
      DO 910 I=(N-1),1,-1
```

```
      X(I)=(B(I)-C(I)*X(I+1))/D(I)
  910 CONTINUE
C     WRITE(*,*)'SOLVETRI OUT OK '
      RETURN
      END
*****************************************************************
*****************************************************************
*****************************************************************
***** Subroutine TOTPRESS
***** -UPDATES THE TOTAL PRESSURE P(I)
***** -UPDATES THE INITIAL VISCOELASTIC CHANGE IN PRESSURE VDP(I)
***** -UPDATES THE INITAL TOTAL VISCOELASTIC CHANGE IN PRESSURE
VP(I)
*****************************************************************
      SUBROUTINE VTOTPRESS(DELTA)
      IMPLICIT REAL*8 (A-H,J,O-Z)
      DIMENSION DELTA(1000)
      COMMON/PARAM/RINC,RIN,ROUT,NLAPS,NINC,NCORE,WT
      COMMON/MATLPROP/EC,E,vc,ET,AA(0:3),ER(1000),vrt,vtr
      COMMON/TIME/R(1000),TIME,TWIND,LAP,DTOLD,DTIME
      COMMON/PRES/P(1000),DP(1000),S,OLDP,VP(1000)
C
      DO I=1,LAP
      P(I)=P(I)+DELTA(I)
      Er(I)=AA(3)*(ABS(P(I)))**3+AA(2)*(ABS(P(I)))**2+AA(1)*
     ' (ABS(P(I)))+AA(0)
      END DO
C
      RETURN
      END
*****************************************************************
*****************************************************************
***** Subroutine OUTS
***** -PRINTS OUPUT OF RADIAL PRESSURES TO THE FILE "OUT.DAT"
*****************************************************************
      SUBROUTINE OUTS
      IMPLICIT REAL*8 (A-H,J,O-Z)
      COMMON/PARAM/RINC,RIN,ROUT,NLAPS,NINC,NCORE,WT
      COMMON/CLOCK/DCLOCK,U(1000),DTP(1000),NCLOCK,J0,J1,T1,J2,T2
      COMMON/MATCOEFF/A(1000),B(1000),C(1000),D(1000),N
      COMMON/MATLPROP/EC,E,vc,ET,AA(0:3),ER(1000),vrt,vtr
      COMMON/TIME/R(1000),TIME,TWIND,LAP,DTOLD,DTIME
      COMMON/PRES/P(1000),DP(1000),S,OLDP,VP(1000)
C
C
```

```
C     WRITE(*,*)'OUTS IN OK '
      PHRASE='**************************************************'
      WRITE(2,20)'   RADIUS        PRESSURE        DELTA'
C     WRITE(5,60)TIME
      DO 9200 I=1,NLAPS+1
      WRITE(2,30)R(I),P(I),DTP(I)
C     WRITE(5,50)R(I),A(I-1),D(I),C(I),B(I)
9200  CONTINUE
      WRITE(4,40)TIME,P(1),DTP(1),B(1),S
C
10    FORMAT(1X,A50)
20    FORMAT(A47,' ',F10.1)
30    FORMAT(F15.4,'   ',F15.8,'      ',E15.8)
40    FORMAT(F10.0,' ',F15.4,' ',E15.8,' ',E15.8,' ',E15.8)
C  50  FORMAT(F8.2,' ',F15.5,' ',F15.5,' ',F15.5,' ',F15.5)
C  60  FORMAT('TIME = ',F10.1)
      RETURN
      END
**********************************************************************
**********************************************************************
***** Subroutine INPUTS
***** -INITIALIZES ALL INPUTS PARAMETERS BY READING
*****  INPUT FILE "CORECRP.IN"
**********************************************************************
      SUBROUTINE INPUTS
      IMPLICIT REAL*8 (A-H,J,O-Z)
      COMMON/PARAM/RINC,RIN,ROUT,NLAPS,NINC,NCORE,WT
      COMMON/CLOCK/DCLOCK,U(1000),DTP(1000),NCLOCK,J0,J1,T1,J2,T2
      COMMON/MATLPROP/EC,E,vc,ET,AA(0:3),ER(1000),vrt,vtr
      COMMON/HUMID/X,HA0,HA1,HA2,HA3,HA4
CCC
C     WRITE(*,*)'ENTER THE WINDING TENSION '
      READ(1,100)WT
C     WRITE(*,*)'ENTER THE INSIDE RADIUS OF THE CORE '
C     READ(1,100)RINC
C     WRITE(*,*)'ENTER THE INSIDE RADIUS OF THE ROLL '
      READ(1,100)RIN
C     WRITE(*,*)'ENTER THE OUTSIDE RADIUS OF THE ROLL '
      READ(1,100)ROUT
C     WRITE(*,*)'ENTER THE RADIAL STIFFNESS OF THE CORE '
      READ(1,120)EC
C     WRITE(*,*)'ENTER THE YOUNGS MODULUS OF THE CORE '
C     READ(1,120)E
C     WRITE(*,*)'ENTER POISSONS RATIO OF THE CORE '
      READ(1,100)vc
```

```
C     WRITE(*,*)'ENTER THE TANGENTIAL MODULUS OF THE ROLL'
      READ(1,100)ET
C     WRITE(*,*)'ENTER THE COEFFICIENTS (c3,c2,c1,c0) OF THE '
C     WRITE(*,*)'RADIAL MODULUS ER=c3*P^2+c2*P^2+c1*P+c0  '
      READ(1,120)AA(3),AA(2),AA(1),AA(0)
C     WRITE(*,*)'ENTER THE POISSONS RATIO vrt OF THE ROLL'
      READ(1,100)vrt
C     WRITE(*,*)'ENTER THE POISSONS RATIO vtr OF THE ROLL'
      READ(1,100)vtr
C
      READ(1,120)J0
C
      READ(1,120)J1
C
      READ(1,120)T1
C
      READ(1,120)J2
C
      READ(1,120)T2
C
C     WRITE(*,*)'ENTER THE TOTAL NUMBER OF LAPS TO BE WOUND '
      READ(1,110)NLAPS
C     WRITE(*,*)'ENTER NUMBER OF CORE SEGMENTS (FOR DISPL FORM)'
C     READ(1,110)NCORE
C     WRITE(*,*)'ENTER THE CHANGE IN TIME '
      READ(1,100)DCLOCK
C     WRITE(*,*)'ENTER THE NUMBER TIME INCREMENTS'
      READ(1,110)NCLOCK
C     WRITE(*,*)'ENTER MOISTURE CONTENT CHANGE CORE WILL
EXPERIENCE'
      READ(1,120)X
C     WRITE(*,*)'ENTER HUMIDITY COMPLIANCE FUNCTION
(H4,H3,H2,H1,H0)'
C     WRITE(*,*)'H(t)=H4*t^4+H3*t^3+H2*t^2+H1*t+H0'
      READ(1,120)HA4,HA3,HA2,HA1,HA0


100   FORMAT(F12.4)
110   FORMAT(I9)
120   FORMAT(E12.5)
      CLOSE(1)
130   continue
      RETURN
      END
*****************************************************************
```

```
**********************************************************************
***** Subroutine UINPUTS
***** -INITIALIZES ALL INPUTS PARAMETERS BY READING
*****  KEYBOARD ENTRY
**********************************************************************
      SUBROUTINE UINPUTS
      IMPLICIT REAL*8 (A-H,J,O-Z)
      COMMON/PARAM/RINC,RIN,ROUT,NLAPS,NINC,NCORE,WT
      COMMON/CLOCK/DCLOCK,U(1000),DTP(1000),NCLOCK,J0,J1,T1,J2,T2
      COMMON/MATLPROP/EC,E,v,ET,AA(0:3),ER(1000),vrt,vtr
      COMMON/HUMID/X,HA0,HA1,HA2,HA3,HA4
CCC

      WRITE(*,*)'ENTER THE WINDING TENSION '
      READ(*,100)WT
      WRITE(1,100)WT
C     WRITE(*,*)'ENTER THE INSIDE RADIUS OF THE CORE '
C     READ(*,100)RINC
C     WRITE(1,100)RINC
      WRITE(*,*)'ENTER THE INSIDE RADIUS OF THE ROLL '
      READ(*,100)RIN
      WRITE(1,100)RIN
      WRITE(*,*)'ENTER THE OUTSIDE RADIUS OF THE ROLL '
      READ(*,100)ROUT
      WRITE(1,100)ROUT
      WRITE(*,*)'ENTER THE RADIAL STIFFNESS OF THE CORE '
      READ(*,120)EC
      WRITE(1,120)EC
C     WRITE(*,*)'ENTER THE YOUNGS MODULUS OF THE CORE '
C     READ(*,120)E
C     WRITE(1,120)E
      WRITE(*,*)'ENTER POISSONS RATIO OF THE CORE '
      READ(*,100)vc
      WRITE(1,100)vc
      WRITE(*,*)'ENTER THE TANGENTIAL MODULUS OF THE ROLL'
      READ(*,100)ET
      WRITE(1,100)ET
      WRITE(*,*)'ENTER THE COEFFICIENTS (c3,c2,c1,c0) OF THE '
      WRITE(*,*)'RADIAL MODULUS ER=c3*P^3+c2*P^2+c1*P+c0  '
      READ(*,120)AA(3),AA(2),AA(1),AA(0)
      WRITE(1,120)AA(3),AA(2),AA(1),AA(0)
      WRITE(*,*)'ENTER THE POISSONS RATIO vrt OF THE ROLL'
      READ(*,100)vrt
      WRITE(1,100)vrt
```

```
      WRITE(*,*)'ENTER THE POISSONS RATIO vtr OF THE ROLL'
      READ(*,100)vtr
      WRITE(1,100)vtr
      WRITE(*,*)'ENTER THE CREEP FUNCTION COEFFICIENTS'
      WRITE(*,*)'J=JO+JI*EXP(-t/T1)+J2*EXP(-t/T2)'
      WRITE(*,*)'JO'
      READ(*,120)J0
      WRITE(1,120)J0
      WRITE(*,*)'J1'
      READ(*,120)J1
      WRITE(1,120)J1
      WRITE(*,*)'T1'
      READ(*,120)T1
      WRITE(1,120)T1
      WRITE(*,*)'J2'
      READ(*,120)J2
      WRITE(1,120)J2
      WRITE(*,*)'T2'
      READ(*,120)T2
      WRITE(1,120)T2
      WRITE(*,*)'ENTER THE TOTAL NUMBER OF LAPS TO BE WOUND < 1000'
      READ(*,110)NLAPS
      WRITE(1,110)NLAPS
C     WRITE(*,*)'ENTER NUMBER OF CORE SEGMENTS (FOR DISPL FORM)'
C     READ(*,110)NCORE
C     WRITE(1,110)NCORE
      WRITE(*,*)'ENTER THE CHANGE IN TIME '
      READ(*,100)DCLOCK
      WRITE(1,100)DCLOCK
      WRITE(*,*)'ENTER THE NUMBER TIME INCREMENTS'
      READ(*,110)NCLOCK
      WRITE(1,110)NCLOCK
      WRITE(*,*)'ENTER MOISTURE CONTENT CHANGE CORE WILL
EXPERIENCE'
      READ(*,120)X
      WRITE(1,120)X
      WRITE(*,*)'ENTER HUMIDITY COMPLIANCE FUNCTION (H4,H3,H2,H1,H0)'
      WRITE(*,*)'H(t)=H4*t^4+H3*t^3+H2*t^2+H1*t+H0'
      READ(*,120)HA4,HA3,HA2,HA1,HA0
      WRITE(1,120)HA4,HA3,HA2,HA1,HA0

100   FORMAT(F12.4)
110   FORMAT(I9)
120   FORMAT(E12.5)
      CLOSE(1)
```

```
130  continue
     RETURN
     END
************************************************************************
************************************************************************
**
***** Subroutine Winder
***** -similar to standard elastic finite difference winding routines
***** -determines the change in radial pressure at radial increment
*****  due to the addition of each layer
***** -store these values in the array DP(layer,layer)
**
************************************************************************
     SUBROUTINE WINDER
     IMPLICIT REAL*8 (A-H,J,O-Z)
     COMMON/PARAM/RINC,RIN,ROUT,NLAPS,NINC,NCORE,WT
     COMMON/CLOCK/DCLOCK,U(1000),DTP(1000),NCLOCK,J0,J1,T1,J2,T2
     COMMON/MATLPROP/EC,E,vc,ET,AA(0:3),ER(1000),vrt,vtr
     COMMON/TIME/R(1000),TIME,TWIND,LAP,DTOLD,DTIME
     COMMON/MATCOEFF/A(1000),B(1000),C(1000),D(1000),N
     COMMON/PRES/P(1000),DP(1000),S,OLDP,VP(1000)
     COMMON/TRY/AA1,BB1,CC1,RK
C
CCCCC CALCULATE INITIAL PRESSURES
C
C    WT=100.0
C    Ec=E*(rin**2-rinc**2)/(rin**2+rinc**2-vc*(rin**2-rinc**2))/rin
C
C    WRITE(*,*)'WINDER IN OK'
     H=(ROUT-RIN)/NLAPS
     R(1)=RIN
     LAP=1
     DO I=2,NLAPS+1
     R(I)=R(1)+(I-1)*H
     END DO
C
CCCCC WIND FIRST LAP
C    WRITE(*,*)'ONE'
C
     LAP=1
C    I=1
     DT=EC*WT*RIN**2/(EC*R(1)**2+H*ET)
C    DT=WT
     DP(1)=(-DT*H)/R(1)
     CALL TOTPRESS(DP)
```

```
C     P(1)=-WT*H/R(1)
C     Er(I)=AA(3)*(ABS(P(I)))**3+AA(2)*(ABS(P(I)))**2+AA(1)*
C    ' (ABS(P(I)))+AA(0)

C
CCCCC  WIND ON SECOND LAP
C
C     WRITE(*,*)'TWO'
      LAP=LAP+1
      I=LAP
      D(1)=(1D0-vrt-Et/(Ec*RIN)-RIN/H)
      C(1)=R(1)/H
      B(1)=0D0
      DP(2)=(-WT*H)/R(LAP)
      DP(1)=(B(1)-DP(2)*C(1))/D(1)
      CALL TOTPRESS(DP)
C     RK=1D0+H*(ET/EC-1D0+vrt)
C     P(2)=-WT*H/R(LAP)
C     P(1)=P(1)+P(2)/RK
C     Er(I)=AA(3)*(ABS(P(I)))**3+AA(2)*(ABS(P(I)))**2+AA(1)*
C    ' (ABS(P(I)))+AA(0)

C
CCCCC  WIND ON LAP THREE
C     WRITE(*,*)'THREE',R(3)
C
C     LAP=3
C     I=LAP
C     P(3)=-WT*H/R(3)
C     AA1=1-(3D0*H)/(2D0*R(2))
C     WRITE(*,*)'AA1'
C     BB1=((H**2)/(R(2)**2))*(1D0-ET/ER(2))-2D0
C     WRITE(*,*)'BB1'
C     CC1=1D0+(3D0*H)/(2D0*R(2))
C     WRITE(*,*)'CC1'
C     DP(1)=CC1*P(3)/(-RK*BB1-AA1)
C     WRITE(*,*)'DP1'
C     DP(2)=RK*DP(1)
C     P(1)=P(1)+DP(1)
C     P(2)=P(2)+DP(2)
C     Er(I)=AA(3)*(ABS(P(I)))**3+AA(2)*(ABS(P(I)))**2+AA(1)*
C    ' (ABS(P(I)))+AA(0)


CCCCC  WIND ON ALL REMAINING LAPS
```

```
C
      DO 50 M=3,NLAPS
      LAP=M
C
      D(1)=1D0-vrt-Et/(Ec*RIN)-RIN/H
      C(1)=R(1)/H
      B(1)=0D0
C
      DO I=2, LAP-1
      A(I-1)=(R(I)**2/H**2-3D0*R(I)/(2D0*H))
      D(I)=(1D0-2D0*R(I)**2/H**2-Et/Er(I))
      C(I)=R(I)**2/H**2+3D0*R(I)/(2D0*H)
      B(I)=0D0
      END DO
C
      DP(LAP)=(-WT*H)/R(LAP)
      B(LAP)=DP(LAP)
      D(LAP)=1D0
      A(LAP-1)=0D0
C
C     WRITE(5,200)TIME
C     DO I=1,LAP
C         WRITE(5,210)R(I),A(I-1),D(I),C(I),B(I)
C     ENDDO
C
      CALL SOLVETRI(DP,LAP)
      CALL TOTPRESS(DP)
50    CONTINUE
C   210FORMAT(F8.2,' ',F15.5,' ',F15.5,' ',F15.5,' ',F15.5)
C   200FORMAT('TIME = ',F10.1)
      CALL OUTS
C     WRITE(*,*)'WINDER OUT OK'
      RETURN
      END
**********************************************************************
**********************************************************************
**********************************************************************
**********************************************************************
***** Subroutine TOTPRESS
***** -UPDATES THE TOTAL PRESSURE P(I)
***** -UPDATES THE INITIAL VISCOELASTIC CHANGE IN PRESSURE VDP(I)
***** -UPDATES THE INITAL TOTAL VISCOELASTIC CHANGE IN PRESSURE
VP(I)
**********************************************************************
      SUBROUTINE TOTPRESS(DELTA)
```

```
      IMPLICIT REAL*8 (A-H,J,O-Z)
      DIMENSION DELTA(1000)
      COMMON/PARAM/RINC,RIN,ROUT,NLAPS,NINC,NCORE,WT
      COMMON/MATLPROP/EC,E,vc,ET,AA(0:3),ER(1000),vrt,vtr
      COMMON/TIME/R(1000),TIME,TWIND,LAP,DTOLD,DTIME
      COMMON/PRES/P(1000),DP(1000),S,OLDP,VP(1000)
C
      DO I=1,LAP
      P(I)=P(I)+DELTA(I)
      Er(I)=AA(3)*(ABS(P(I)))**3+AA(2)*(ABS(P(I)))**2+AA(1)*
     ' (ABS(P(I)))+AA(0)
      END DO
C
      RETURN
      END
*********************************************************************
*********************************************************************
*********************************************************************
*********************************************************************
*********************************************************************
***** Subroutine POUT
***** output pressure to be use in other program
*********************************************************************
      SUBROUTINE POUT
      IMPLICIT REAL*8 (A-H,J,O-Z)
      COMMON/TIME/R(1000),TIME,TWIND,LAP,DTOLD,DTIME
      COMMON/MATLPROP/EC,E,vc,ET,AA(0:3),ER(1000),vrt,vtr
      COMMON/PRES/P(1000),DP(1000),S,OLDP,VP(1000)
      COMMON/PARAM/RINC,RIN,ROUT,NLAPS,NINC,NCORE,WT
C
C
C
      DO 1100 I=1,NLAPS+1
      WRITE(5,70) Er(I),P(I),R(I)
70    FORMAT(F15.8,F15.8,F15.4)
1100  CONTINUE
      RETURN
      END
*********************************************************************
```

VITA

Hung Nguyen

Candidate for the Degree of

Master of Science

Thesis: HYGROSCOPIC EFFECTS ON PAPERBOARD CORES AND WOUND ROLLS

Major Field: Mechanical Engineering

Biographical:

Personal Data: Born in Saigon, Vietnam, on June 12, 1973, the son of Son and Que Nguyen

Education: Graduated from Edmond Memorial High School, Edmond, Oklahoma in May 1991; receive Bachelor of Science degree in Mechanical Engineering from Oklahoma State University, Stillwater, Oklahoma in December 1995. Complete the requirements for the Master of Science degree with a major in Mechanical Engineering at Oklahoma State University in December, 1997.

Experience: Employed as an engineer intern for ASARCO. Research Assistant, Department of Mechanical and Aerospace Engineering, Oklahoma State University, January, 1996 to August, 1997.

Professional Memberships: Pi Tau Sigma